



Université Mohamed Khider de Biskra
Faculté de science et technologie
Département de génie mécanique.

MÉMOIRE DE MASTER

Domaine : Sciences et Techniques

Filière : Génie Mécanique

Spécialité : Construction Mécanique

Réf. : Entrez la référence du document

Présenté et soutenu par :
Ayoub MACHIOURI, Manar GUITOUN

Le : mercredi 22 juin 2022

Contribution to the numerical and experimental modeling of the thermo-elastic behavior of materials based on porous textures: Application to dental restoration.

Jury :

| | | | | |
|-----|----------------|-----|----------------------|------------|
| Pr. | Mabrouk HECINI | Pr | Université de Biskra | Président |
| Pr. | Lakhdar SEDIRA | Pr | Université de Biskra | Rapporteur |
| Dr. | Tarek DJOUDI | MCA | Université de Biskra | Examineur |

Dedication

TO ME.

Ayoub MACHIOURI

Dedication

I would like to give special thanks

**My dear mother and heroine, my dear father, to my wonderful
sisters, To my dear brothers, to my dear fiancé**

To all my friends without exception

for all my family

To everyone who loves me from near or far....

Manar GUITOUN

List Of Figures.

Chapter I. Bibliographic studies: background and generality.

| | |
|--|----|
| Figure I. 1.Schematic representation of dental structural organization[2]. | 4 |
| Figure I. 2.Classification of porous materials based on pore size. | 8 |
| Figure I. 3.A homogeneous structure made of a heterogeneous material. | 10 |
| Figure I. 4.The linear Triangular Element T3. | 13 |

Chapter II. Mechanical and chemical characterization of dental materials.

| | |
|---|----|
| Figure II. 1.Experimental plan of work. | 19 |
| Figure II. 2. Crop view of natural tooth shows different layers. | 20 |
| Figure II. 3.Demonstration of the zone where the specimens are taken. | 21 |
| Figure II. 4. Natural dental tissue specimens for A) compressive testing and B) hardness testing. | 21 |
| Figure II. 5 IPS d.SIGN A) original flask B) raw powder. | 22 |
| Figure II. 6. Microscopic imaging of IPS d.SIGN powder A) $\times 10$ B) $\times 20$ C) $\times 40$ D) $\times 100$. | 23 |
| Figure II. 7.Method of preparation(A) and string(B) of IPS d.SIGN. | 24 |
| Figure II. 8. IPS d.SIGN specimens for A) compressive testing B) hardness testing. | 25 |
| Figure II. 9. A) indentation shape of Vickers hardness test B) Hardness testing machine (INNOVATEST). | 26 |
| Figure II. 10.A) Compressive test machine Instron 5969, B) Specimen under compressive forces. | 27 |
| Figure II. 11.Vickers hardness test results on dentin specimen S4. | 28 |
| Figure II. 12.Stress-strain curve of compressive test on natural Dentin. | 31 |
| Figure II. 13. Stress-strain curve of compressive test on IPS d.SIGN. | 32 |
| Figure II. 14. XRD curve results for natural dentin. | 34 |
| Figure II. 15. XRD curve results for IPS d.SIGN powder. | 35 |
| Figure II. 16. XRD curve results for IPS d.SIGN solid. | 35 |

Chapter III. Numerical modeling of the thermo-elastic behavior of porous materials.

| | |
|---|----|
| Figure III. 1. A) RSE generated by MATLAB B) inclusion phase treated as void C) inclusion phase treated as air..... | 39 |
| Figure III. 2.The RSE of IPS e.max CAD (A) raw micro-CT scan picture (B) treated picture (binarized)..... | 40 |
| Figure III. 3. IPS d.SIGN microscopic images size of A) raw B) binarized. | 40 |
| Figure III. 4.The effect of the Poison's ratio of air on Poison's ratio of air of porous Titanium. | 43 |
| Figure III. 5.The effect of the elastic property of air on Young's modulus of porous Titanium. | 43 |
| Figure III. 6. Meshed microstructure for (A) IPS e.max CAD (B) IPS d.SIGN | 44 |
| Figure III. 7. State of stress of (A) IPS e.max CAD (B) IPS d.SIGN, using COMSOL. | 44 |
| Figure III. 8. State of strain of (A) IPS e.max CAD (B) IPS d.SIGN using COMSOL. | 45 |
| Figure III. 9. State of displacement magnitude for A) IPS e.max CAD B) IPS d.SIGN, using COMSOL. | 46 |
| Figure III. 10. State of Von-Mises stresses for A) IPS e.max CAD B) IPS d.SIGN, using COMSOL. | 47 |

Chapter IV. Numerical 3D modeling of the thermo-elastic behavior of restorative materials

| | |
|--|----|
| Figure IV. 1. Simplified premolar tooth model geometry..... | 51 |
| Figure IV. 2. Complete mesh of the simplified tooth model. | 52 |
| Figure IV. 3. The simplified tooth model Under boundary load. | 53 |
| Figure IV. 4. The simplified tooth model Under thermal boundary conditions. | 53 |
| Figure IV. 5. Slice evaluation of Von Mises A) Natural enamel B) IPS e.max CAD C) IPS d.SIGN for Mechanical loading..... | 54 |
| Figure IV. 6 Slice evaluation of Von Mises A) Natural enamel B) IPS e.max CAD C) IPS d.SIGN for thermal loading. | 54 |

List Of Tables.

Chapter II. Mechanical and chemical characterization of dental materials.

| | |
|---|----|
| Table II. 1. Hardness test specimens' details..... | 20 |
| Table II. 2. Compressive test specimen sizes (Dentin)..... | 21 |
| Table II. 3. Compressive test specimen IPS d.SIGN sizes. | 24 |
| Table II. 4. Vickers hardness test results. | 28 |
| Table II. 5. Mechanical properties obtained from the compressive testing..... | 30 |

Chapter III. Numerical modeling of the thermo-elastic behavior of porous materials.

| | |
|---|----|
| Table III. 1. IPS e.max CAD composition, mechanical and physical properties. | 38 |
| Table III. 2. Composition of IPS d.SIGN in (w%). | 38 |
| Table III. 3. The thermal and mechanical proprieties of non-porous IPS e.max CAD. | 41 |
| Table III. 4. The thermal and mechanical proprieties of non-porous IPS d.SIGN..... | 42 |
| Table III. 5. Average values for Stress and Strain tensors for the IPS e.max CAD RVE... | 45 |
| Table III. 6. Engineering modulus of the homogenous IPS e.max CAD glass ceramic..... | 46 |
| Table III. 7. Average values for Stress and Strain tensors for the IPS d.SIGN RVE..... | 46 |
| Table III. 8. Engineering modulus of the homogenous IPS d.SIGN glass-ceramic. | 46 |

Chapter IV. Numerical 3D modeling of the thermo-elastic behavior of restorative materials.

| | |
|---|----|
| Table IV. 1. Material properties used in the FEAmoel..... | 51 |
|---|----|

Table of Contents

| | |
|--|------|
| Acknowledgment | I |
| Table of Contents..... | II |
| List of Figures..... | III |
| List of Tables..... | V |
| General Introduction..... | VI |
| Chapter I. Bibliographic studies: background and generality | 1 |
| Chapter II. Mechanical and chemical characterization of dental materials..... | 17 |
| Chapter III. Numerical modeling of the thermo-elastic behavior of porous materials..... | 36 |
| Chapter. IV Numerical 3D modeling of the thermo-elastic behavior of restorative materials..... | 49 |
| General conclusion..... | VIII |
| Abstract..... | |

Dedication

TO ME.

Ayoub MACHIOURI

Dedication

I would like to give special thanks

**My dear mother and heroine, my dear father, to my wonderful
sisters, To my dear brothers, to my dear fiancé**

To all my friends without exception

for all my family

To everyone who loves me from near or far....

Manar GUITOUN

General Introduction

Teeth are among the hardest materials in the human body, and also essential for chewing. That play an important role in the aesthetic appearance of the lower third of the face.

During the start of dental science, dentistry was just an associate art practiced by barber-surgeons or artisans. With time, the information on dentistry had unfolded primarily in France, Germany, Italy, and England. With the arrival of science and technology, dentistry came into the hands of professionally minded dentists/surgeons. Slowly and bit by bit operative dental medicine came out collectively of the major branches of dentistry and dentists started minded on restoring and conserving teeth. With the innovations and discoveries of the latest instrumentality, techniques, materials, and ways, operative dental medicine continues to be enriched, refined, and grow toward a bright future [1].

Ceramic materials for dental restorations were first used in the 18th century .for their Aesthetics (adequate translucency) and durability (adequate strength and chemical stability) which are two attributes of ceramics over other materials [2]. And after the sudden discovery of Glass ceramics [3] in 1953, and the major improvements associated with this new material. Professor Hench.[4] developed biomaterials for dental restorations as lithium disilicate glass-ceramics, opening up a new branch in the restorative dentistry.

In this work, we investigate the thermo-elastic behavior of glass-ceramics intended for dental restoration. The used ceramic is a porous material which is generally considered as a fundamental feature.

The material is prepared in privet Laboratory and experimental tests were conducted in the laboratory of the University of Biskra. Numerical simulations are performed using COMSOL Multiphysics and Digimat software. The purpose of this study can be summarized in three points:

- Broaden the field of knowledge related to the porous glass-ceramics and the restorative dental materials.
- Experimentally studies the thermo-elastic behavior of a composite material subjected to difference of temperature or mechanical loading and compare it with numerical and analytical simulations.
- Assess the macro-mechanical thermo-elastic properties of dental restoration materials.
- Simulate the thermo-mechanical behavior of a tooth prototype.

However, to establish this work, related details are developed in the present manuscript, where four chapters are presented, herein:

Chapter I: This part constitutes a set of definitions for dental biomaterials, glass-ceramics, and the concept of porosity in the materials. The thermo-elastic behavior of glass-ceramics and different homogenization methods for characterization of porous material are also presented in this chapter.

Chapter II: The experimental part is presented in chapter II, where the laboratory works includes the elaboration of the material specimens, the mechanical (compression, hardness) and chemical tests (XRD analysis).

Chapter III: Numerical and analytical overviews on modeling of the thermo-elastic behavior of porous glass-ceramics are presented in previous chapter. However, simulation and analyses are performed in chapter III, using the Finite Element Method (FEM) and Mori-Tanaka method to determine the homogeneous properties.

Chapter IV: deals with a numerical application that synthesizes the analysis of structural behavior of a virtual tooth using a glass-ceramic material. In this section, the states of strain and stress of the analyzed structure will be presented highlighting the critical zones.

Finally, a general conclusion is given in the last section. The present work has revealed some difficulties and perspectives that are summarized next.

References

1. Singh, H., et al., *Evolution of restorative dentistry from past to present*. Indian Journal of Dental Sciences, 2017. **9**(1): p. 38.
2. Fu, L., H. Engqvist, and W. Xia, *Glass–ceramics in dentistry: A review*. Materials, 2020. **13**(5): p. 1049.
3. Zanotto, E.D., *Bright future for glass-ceramics*. American Ceramics Society Bulletin, 2010. **89**(8): p. 19-27.
4. Höland, W., et al., *Clinical applications of glass-ceramics in dentistry*. Journal of Materials Science: Materials in Medicine, 2006. **17**(11): p. 1037-1042.

Chapter I.

Bibliographic studies: background and generality.

Table of Contents

| | |
|---|----|
| Chapter I. Bibliographic studies: background and generality. | |
| I. 1. Introduction | 3 |
| I. 2. What is a tooth?..... | 3 |
| I. 3. Structure of teeth | 3 |
| I. 3. 1. Enamel | 4 |
| I. 3. 2. Cementum | 4 |
| I. 3. 3. Dentin..... | 4 |
| I. 3. 4. Pulp | 5 |
| I. 4. Oral cavity | 5 |
| I. 5. Ceramics..... | 5 |
| I. 6. Bio-material..... | 6 |
| I. 6. 1. Ceramics in bio-materials | 6 |
| I. 7. Mechanical properties | 6 |
| I. 7. 1. Strength | 6 |
| I. 7. 2. Elastic Modulus (Young's modulus) | 6 |
| I. 7. 3. Hardness | 7 |
| I. 8. Porous materials | 7 |
| I. 8. 1. Classification of porous materials..... | 7 |
| I. 8. 1. 1. Classification by size..... | 7 |
| I. 8. 1. 2. Classification by shape..... | 8 |
| I. 9. Porous structure analysis..... | 9 |
| I. 10. Representative Volume Element (RVE) | 9 |
| I. 11. Homogenization of composite material | 9 |
| I. 11. 1. Homogenization methods | 10 |
| I. 11. 2. Analytic method of Mori-Tanaka | 10 |
| I. 11. 3. Numerical method (Finite Elements Method) | 11 |
| I. 11. 3. 1. Three nodes triangle membrane element T3 | 12 |
| I. 12. Modeling of thermo-elastic behavior | 14 |
| I. 12. 1. Formulation and constitutive equation..... | 14 |
| I. 12. 2. Thermo-elasticity | 14 |
| I. 13. Conclusion..... | 15 |
| References | 16 |

I. 1. Introduction

Due to the great development of materials science and manufacturing techniques, the world had, during the late 19th and early 20th centuries, a leap in the field of dental restoration materials. The improvement was not limited to ensuring proper functioning, but took into account the aesthetic aspect of the restored tooth [1].

In this chapter, we aim to introduce a general view on the natural dental tissue, as well as the porous biomaterials and their role in the restoration of the decayed and damaged dental tissue. Some theoretical details concerning the modeling of the thermo-mechanical behavior have also been described in this chapter. We emphasize analytical and numerical approaches in the characterization of heterogeneous materials.

I. 2. What is a tooth?

The definition of a tooth according to Britannica [2] is, any of the hard, resistant structures occurring on the jaws and in/or around the mouth and pharynx areas of vertebrates. Teeth are multi-purpose objects mainly for catching and masticating food, for defense, and other specialized uses.

A tooth made of a crown and one or more roots. The crown is the active part that is visible above the gum. The root is the hidden part that supports and holds the tooth in the jawbone.

I. 3. Structure of teeth

The tooth is made up of four tissues: enamel, dentin, cementum, and pulp, **Figure I. 1**. The first three, are fairly hard since they contain a considerable number of mineral substances, mainly calcium. Two of these tissues are normally visible in an intact extracted tooth: enamel and cementum. The others are usually not visible on an intact tooth [3].

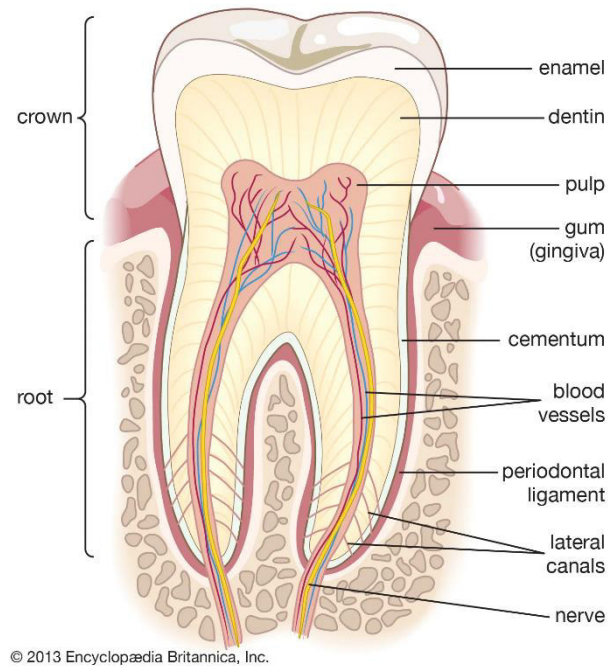


Figure I. 1. Schematic representation of dental structural organization[2].

I. 3. 1. Enamel

Enamel is the protective external surface layer of the crown. It is highly calcified or mineralized and is the hardest substance in the body. Its mineral content is 90% calcium hydroxyapatite. The remaining substances include water and enamel matrix [3].

I. 3. 2. Cementum

The cementum is the external layer of the tooth root. The cementum is very thin, especially next to the cervical line, (only 50–100 μm .) Cementum is about as hard as bone but considerably softer than enamel. It develops from the dental sac (mesoderm) and is produced by cells called cementoblasts. The cemento-enamel junction (also called the CEJ) separates the enamel of the crown from the cementum of the anatomic root. This junction is also known as the cervical line, denoting that it surrounds the neck or cervix of the tooth of specialized epithelial cells called ameloblasts [3].

I. 3. 3. Dentin

Dentin is the hard yellowish tissue under the enamel and cementum and makes up the major bulk of the inner portion of each tooth crown and root. It extends from the pulp cavity in the center of the tooth outward to the inner surface of the enamel (on the crown) or cementum (on the root) [3].

Dentin is not normally visible except on a dental radiograph, or when the enamel or cementum has been worn away, or cut away when preparing a tooth with a bur or destroyed by decay. Mature dentin is composed of about 70% calcium hydroxyapatite, 18% organic matter (collagen fibers), and 12% water, making it harder than cementum but softer and less brittle than enamel[3].

I. 3. 4. Pulp

Pulp is the soft (not calcified or mineralized) tissue in the cavity or space in the center of the crown and root called the pulp cavity. The pulp cavity has a coronal portion (pulp chamber) and a root portion (pulp canal or root canal). The pulp cavity is surrounded by dentin, except at a hole (or holes) near the root tip (apex) called an apical foramen (plural foramina). Nerves and blood vessels enter the pulp through apical foramina. Like dentin, the pulp is normally not visible. Pulp is soft connective tissue containing a rich supply of blood vessels and nerves [3].

I. 4. Oral cavity

The oral cavity is a very complex and aggressive environment for any materials to be in, natural tissues or reconstructive materials alike, therefore Bradna et Al.[4] has established a list of potential environmental agents that can affect their contents :

- Saliva, water, enzymes, ions.
- Plaque, bacteria, and products of their metabolism (organic acids like acetic, formic, propionic, lactic. decreasing pH even to 4.5).
- Changes in pH and temperature.

pH: 6.5-6.9 (normal level); 7.0-7.5 (after stimulation) and body temperature is 37 C°

- Food components, exogenous and endogenous chemical substances Drinks such as “soft drinks “with a high content of organic acids (pH frequently below 2.0, citric, phosphoric acids) and simple saccharides, energetic drinks, foodstuff, and sweets.
- Mechanical stresses. Forces during chewing/biting 100-400 N (up to app. 50-200 MPa), compressive, tensile, flexural, or shear

I. 5. Ceramics

Ceramics have various definitions, because of their long history of development as one of the oldest and most versatile groups of materials and because of the different ways in which materials can be classified, such as by chemical composition (silicates, oxides, and non-

oxides), properties (mechanical and physical), or applications (building materials, high-temperature materials, and functional materials). The most widely used, minimal definition of ceramics is “**that they are inorganic nonmetallic materials**”.[4]

I. 6. Bio-material

Biomaterial is a substance that has been engineered to take a form which alone or as a part of a complex system, and have a direct interaction with components of living systems, without any therapeutic or diagnostic procedure [5]. Biomaterials take the form of implants (dental implants, heart valves, intraocular lenses, ligaments, vascular grafts, etc.) or medical devices (artificial hearts, biosensors, pacemakers, etc.).

The properties of biomaterials used in regenerative medicine largely depend on the properties of the material used for their preparation (polymer, ceramic, metal, carbon, or their combination as composite material); forms: solid material, porous material; spatial construction as well as physical and chemical properties [5].

I. 6. 1. Ceramics in bio-materials

Ceramics are polycrystalline materials. They are very brittle, sensitive to the presence of cracks or other defects, and have poor resistance against tension forces. As a result, they are used less extensively than either metals or polymers. On the other hand, they exhibit hardness, great strength, stiffness, low density, and are resistant to wear and corrosion. Ceramics are usually electrical and thermal insulators[5].

I. 7. Mechanical properties

I. 7. 1. Strength

This value describes the magnitude of stress at which the material begins to fracture, the field of strength of materials deals with forces and deformations that outcomes from their acting on a material. A load applied to a mechanical part will incite interior forces inside the part called stresses when those forces are applied. The stresses following up on the material causes deformation of the material in different manners including breaking them. Deformation of the material is called strain.

I. 7. 2. Elastic Modulus (Young’s modulus)

The ratio between stress and strain in the elastic region is Young's modulus, also called the modulus of elasticity, which we denote with the letter E. It has the same units as stress, so. We can also measure Young's modulus as the gradient of the slope in the elastic region.

Young's modulus is essentially a measure of how stiff a material is, the higher Young's modulus, the stiffer of material and so the smaller the elastic deformations will be for a given applied load.

I. 7. 3. Hardness

Hardness (H) is a measure of a material's resistance to deformation by surface indentation. The plastic deformation is caused by the motion of dislocations in the atomic structure of a material.

I. 8. Porous materials

A porous medium is a two-phase heterogeneous material consisting of a solid phase and a void phase called a "pore". On a global scale, these materials are characterized as a continuous medium by introducing the effect of porosity. This porosity can take different forms such as spherical, elongated, flattened, etc.

Generally, porous materials contain a porosity of 0.2-0.95. The porosity is an expression of the fraction of pore volume to the total volume [6].

I. 8. 1. Classification of porous materials

It is difficult to give a consistent classification of porous materials, so we have two main classifications made, either by porous size or structure:

I. 8. 1. 1. Classification by size

The International Union of Pure and Applied Chemistry (IUPAC¹) has recommended a classification by pores size [7]. The classification of porous materials by pore size is shown in the **Figure I. 2:**

- Microporous: pore diameter < 2 nm
- Mesoporous: 2 nm < pore diameter < 50 nm
- Macroporous: 50 nm < pore diameter

¹ The International Union of Pure and Applied Chemistry (IUPAC) is the world authority on chemical nomenclature and terminology, including the naming of new elements in the periodic table; on standardized methods for measurement; and on atomic weights, and many other critically-evaluated data.

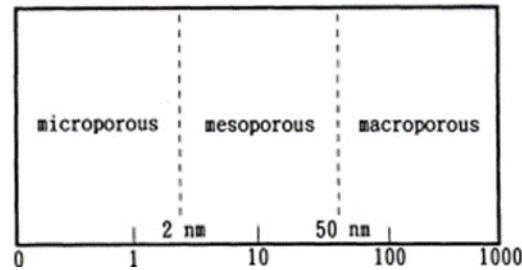


Figure I. 2. Classification of porous materials based on pore size [7].

I. 8. 1. 2. Classification by shape

Bargmann et al.[8] introduce the following classification for porous solids, partly based on the definitions and terminology of Rouquerol et al. [9]:

- Agglomerates

Rouquerol considers porous materials which are consolidated, existing as relatively rigid, macroscopic bodies whose dimensions exceed those of the pores by many orders of magnitude. They divide these into two groups depending on the relative density. Materials with relative density smaller than 0.3 are referred to as cellular materials.

- Cellular structures:

A cellular solid is one made up of an interconnected network of solid struts or plates which form the edges and faces of cells. This group also can be sub divided in 2 small groups [6].

- ❖ Closed-cell structures:

Open cell structure has tiny cells which are not completely closed the open cells are filled with air and this affects the way the materials perform.

- ❖ Open-cell structures:

Closed cell structure has cells which are sealed off so air doesn't get inside the structure at all.

- Matrix-dilute pore systems:

Matrix-dilute pore material systems consist of a matrix material which contains isolated voids.

- Aggregates, such as sand, crushed stone, recycled concrete:

we consider unconsolidated, non-rigid, more-or-less loosely packed assemblages of individual particles where the particles are surrounded by a network of interparticle voids whose volume fraction may be as large as 80% [8].

I. 9. Porous structure analysis

The structure of most porous media is far too irregular and complicated to allow a rigorously correct geometrical description. Even if it is possible somehow to enter all pores with a tiny probe and determine the coordinates of every point on the bounding surfaces of the pores and store this information in the memory of some giant computer, this kind of three-dimensional map of the pore structure would only be of limited usefulness [10].

The description of a material must be sufficiently rich and realistic to correctly estimate the porous material behaviors. For this, we seek the sufficient size and geometric description of the representative structure for the property that we wish to estimate. We are talking here about RVE (Representative Volume Element).

I. 10. Representative Volume Element (RVE)

The Representative Elementary Volume (RVE) plays an important role in the mechanics and physics of random heterogeneous media in order to determine their effective properties[11].

Choosing a good RVE is crucial for the estimation of the global response in a heterogeneous material. The knowledge of the size of the RVE represents an essential element for the determination of the effective properties. This size depends on the nature and constituents of the material.

It is thus possible to define a Representative Volume Element of the heterogeneous material. This must be characteristic of the microstructure of the material. It is then replaced by an Equivalent Homogeneous Media (EHM) which is none other than a medium having the same effective properties as the RVE. It can therefore in any case represent the material.

I. 11. Homogenization of composite material

Composite materials are formed from at least two materials. They can be more or less complex. They consist of different phases (materials) which have their own characteristics. Heterogeneous medium can be very difficult and computationally expensive. First of all, there are two aspects for homogenization, analytical one and numerical one. For the numerical we have to know how to mesh with precision the structure and then know how to manage the boundary conditions which are applied. This is why it is interesting to homogenize. It's about finding an equivalent material which exhibits, macroscopically, the behavior composite mechanics [12].

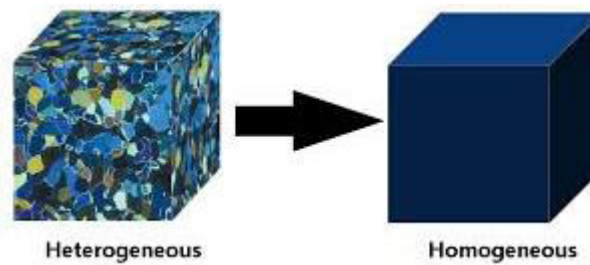


Figure I. 3. A homogeneous structure made of a heterogeneous material.

I. 11. 1. Homogenization methods

We are interested in methods for evaluating the homogenized elasticity tensor, there are two types of methods:

- Mean Field Methods;
- Full Field Methods.

The latter require a complete knowledge of the microstructure, we speak of a numerical approach for the calculation of homogenized elasticity tensor, when the whole of the microstructure is identified, the stress and strain tensors can then be calculated at any point of the microstructure using methods based on finite elements or fast Fourier transform (FFT). Using partial knowledge of the microstructure, mean-field methods apply in the case where full-field methods do not may apply (lack of information on the microstructure). We then speak of an approach analytic [13].

I. 11. 2. Analytic method of Mori-Tanaka

In 1973, Mori-Tanaka proposed a rational approach to correlate averaged stresses and strains of the constituent fiber with those of the matrix in a composite. Later in 1987, Benveniste found that the Mori-Tanaka's approach can be reformulated by making use of the equivalent inclusion idea in terms of a more compacted tensor, which is called the Mori-Tanaka's tensor here and in the following. This tensor in a way only depends on an Eshelby's tensor. From this tensor, all of the effective elastic properties of the composite can be determined. Thus far, the Eshelby-Mori-Tanaka's method has become very popular in the composite community. Moreover, a lot of work has been done to study mechanical behaviors of hybrid composites containing various kinds of inclusion shapes, including ellipsoidal family with different aspect ratios, from penny-shaped disc, spherical inclusion, to non-circular cylinder reinforcement [14].

Mori-Tanaka method is briefly discussed here for N-phase composites. The strain ε_r in the r-th phase is connected with the average macroscopic strain $\bar{\varepsilon}$ through the localization equation:

$$\varepsilon_r = A_r : \bar{\varepsilon} \quad \text{I. 1}$$

The strain concentration tensor A_r is obtained by the relation:

$$A_r = T_r : \left[\sum_{n=0}^N c_n T_n \right]^{-1} \quad \text{I. 2}$$

where c_r denotes the volume fraction of the r-th phase and T_r is the interaction tensor expressed as:

$$A_r = T_r : \left[I + S(C_0) : C_0^{-1} : [C_r - C_0] \right]^{-1} \quad \text{I. 3}$$

It is recalled that I is the fourth order symmetric identity tensor. $S(C_0)$ denotes the Eshelby tensor which depends on the properties of the matrix (matrix stiffness tensor C , as well as the ellipsoidal geometry of the fiber (form factor)). Considering the elastic modulus C_r of each phase r, as well as the concentration tensors A_r , the overall macroscopic elastic stiffness \bar{C} is computed as follows:

$$\bar{C} = \sum_{r=0}^N c_r C_r : A_r \quad \text{I. 4}$$

The last expression is suitable for elastic materials. For inelastic phases, the incremental methods propose to substitute the elastic modulus C by the tangent modulus L^t [15].

I. 11. 3. Numerical method (Finite Elements Method)

In engineering problems there are some basic unknowns. If they are found, the behavior of the entire structure can be predicted. The basic unknowns or the Field variables which are encountered in the engineering problems are displacements in solid mechanics, velocities in fluid mechanics, electric and magnetic potentials in electrical engineering and temperatures in heat flow problems. In a continuum, these unknowns are infinite. The finite element procedure reduces such unknowns to a finite number by dividing the solution region into small parts called elements and by expressing the unknown field variables in terms of assumed approximating functions (Interpolating functions/Shape functions) within each element. The approximating functions are defined in terms of field variables of specified

points called nodes or nodal points. Thus, in the finite element analysis the unknowns are the field variables of the nodal points. Once these are found the field variables at any point can be found by using interpolation functions. After selecting elements and nodal unknowns next step in finite element analysis is to assemble element properties for each element. For example, in solid mechanics, we have to find the force-displacement i.e., stiffness characteristics of each individual element. Mathematically this relationship is of the form:

$$[k]_e \{\delta\}_e = [F]_e \quad \text{I. 5}$$

Where $[k]_e$ is element stiffness matrix, $\{\delta\}_e$ is nodal displacement vector of the element and $[F]_e$ is nodal force vector [16].

There exist several families of elements to make the discretization of the structure, we can find elements with triangular base, the linear triangle T3, quadratic triangle T6 and the linear tetrahedron T4, and the elements with quadrangular base Q4 (bilinear Quadrangle 4 nodes), Q8 (incomplete quadratic quadrangle 8 nodes) and the Q9 (complete quadratic quadrangle 9 nodes).

I. 11. 3. 1. Three nodes triangle membrane element T3

The linear triangular element is a two-dimensional finite element with both local and global coordinates. It is characterized by Linear shape functions. This element can be used for plane stress or plane strain problems in elasticity, it is also called the constant strain triangle. The linear triangular element has modulus of elasticity E , Poisson 's ratio ν and thickness. Each linear triangle has three nodes with two in-plane degrees of freedom at each node as shown in **Figure I. 4**.

The global coordinates of the three nodes are denoted by (x_i, y_i) , (x_j, y_j) , and (x_m, y_m) . The order of the nodes for each element is important clockwise direction starting from any node [17].

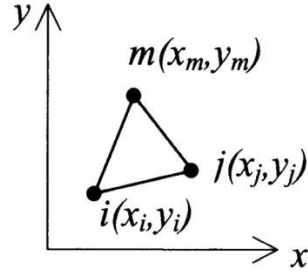


Figure I. 4.The linear Triangular Element T3.

$$[k] = tA[B]^T[D][B] \quad \text{I. 6}$$

where A is the area of the element given by:

$$2A = x_i(y_j - y_m) + x_j(y_m - y_i) + x_m(y_i - y_j) \quad \text{I. 7}$$

and the matrix [B] is given by:

$$[B] = \frac{1}{2A} \begin{bmatrix} \beta_i & 0 & \beta_j & 0 & \beta_m & 0 \\ 0 & \gamma_i & 0 & \gamma_j & 0 & \gamma_m \\ \gamma_i & \beta_i & \gamma_j & \beta_j & \gamma_m & \beta_m \end{bmatrix} \quad \text{I. 8}$$

Where $\beta_i, \beta_j, \beta_m, \gamma_i, \gamma_j, \gamma_m$ are given by:

$$\begin{aligned} \beta_i &= y_j - y_m \\ \beta_j &= y_m - y_i \\ \beta_m &= y_i - y_j \\ \gamma_i &= x_m - x_j \\ \gamma_j &= x_i - x_m \\ \gamma_m &= x_j - x_i \end{aligned} \quad \text{I. 9}$$

For cases of plane stress, the matrix [D] is given by:

$$[D] = \frac{E}{1-\nu^2} \begin{bmatrix} 1 & \nu & 0 \\ \nu & 1 & 0 \\ 0 & 0 & \frac{(1-\nu)}{2} \end{bmatrix} \quad \text{I. 10}$$

For cases of plane strain the matrix [D] is given by:

$$[D] = \frac{E}{(1+\nu)(1-2\nu)} \begin{bmatrix} 1-\nu & \nu & 0 \\ \nu & 1-\nu & 0 \\ 0 & 0 & \frac{(1-2\nu)}{2} \end{bmatrix} \quad \text{I. 11}$$

I. 12. Modeling of thermo-elastic behavior

I. 12. 1. Formulation and constitutive equation

Engineer's modules are Young's moduli, Poisson's ratios and shear moduli. These modules are measured in simple tests such as uniaxial tensile or shear tests. These modules therefore correspond to a more practical usual use than the stiffness or flexibility constants. Generally, these tests are carried out by imposing a known stress field, then by calculating the strain field. It follows that the flexibility constants are related to the engineer's modules by simpler relations than those expressing the stiffness constants. We establish these various relations below by considering various fundamental tests.

- Modules Young's modulus: $E_L, E_T, E_{T'}$.
- Poisson ratio: $\nu_{LT}, \nu_{LT'}, \nu_{TT'}$.
- Shear modulus: $G_{LT}, G_{LT'}, G_{TT'}$.

If the material was isotropic these values can be written as following:

$$E_L, E_T, E_{T'}=E, \nu_{LT}, \nu_{LT'}, \nu_{TT'} =\nu, G_{LT}, G_{LT'}, G_{TT'}=G$$

$$\text{Where: } G = \frac{E}{2(1+\nu)}$$

Then the constitutive equation can be written as following [18] :

$$\begin{Bmatrix} \epsilon_x \\ \epsilon_y \\ \epsilon_z \\ \gamma_{yz} \\ \gamma_{xz} \\ \gamma_{xy} \end{Bmatrix} = \begin{bmatrix} \frac{1}{E} & -\frac{\nu}{E} & -\frac{\nu}{E} & 0 & 0 & 0 \\ -\frac{\nu}{E} & \frac{1}{E} & -\frac{\nu}{E} & 0 & 0 & 0 \\ -\frac{\nu}{E} & -\frac{\nu}{E} & \frac{1}{E} & 0 & 0 & 0 \\ 0 & 0 & 0 & \frac{1}{G} & 0 & 0 \\ 0 & 0 & 0 & 0 & \frac{1}{G} & 0 \\ 0 & 0 & 0 & 0 & 0 & \frac{1}{G} \end{bmatrix} \begin{Bmatrix} \sigma_x \\ \sigma_y \\ \sigma_z \\ \tau_{yz} \\ \tau_{xz} \\ \tau_{xy} \end{Bmatrix} \quad \text{I. 12}$$

I. 12. 2. Thermo-elasticity

Most materials tend to expand if their temperature rises and, to a first approximation, the expansion is proportional to the temperature change. If the expansion is unrestrained, all dimensions will expand equally i.e., there will be a uniform dilatation described by:

$$\epsilon_{xx} = \epsilon_{yy} = \epsilon_{zz} = \alpha T \quad \text{I. 13}$$

Where α is the coefficient of linear thermal expansion.

Notice that no shear strains are induced in unrestrained thermal expansion, so that a body which is heated to a uniformly higher temperature will get larger, but will retain the same shape.

Thermal strains are additive to the elastic strains due to local stresses, so that Hooke's law is modified to the form [19] :

$$\epsilon_{xx} = \frac{\sigma_{xx}}{E} - \frac{\nu\sigma_{yy}}{E} - \frac{\nu\sigma_{zz}}{E} + \alpha T \quad \text{I. 14}$$

$$\epsilon_{xy} = \frac{2\sigma_{xy}}{E} (1 + \nu) \quad \text{I. 15}$$

I. 13. Conclusion

In this chapter, we have introduced some definitions concerning teeth and ceramics as a porous bio-material intended for dental restoration. We also presented some details that can be useful for the analysis of the thermo-elastic behavior of porous composite structures, in particular teeth and dental restorative materials. In order to achieve this goal, it should be noted that both analytical and numerical approaches (with Representative element Volume) are detailed and will be used in subsequent sections.

References

1. Singh, H., et al., *Evolution of restorative dentistry from past to present*. Indian Journal of Dental Sciences, 2017. **9**(1): p. 38.
2. Encyclopaedia, T.E.o., *tooth*, in *Encyclopedia Britannica*2021.
3. Scheid, R.C., *Woelfel's dental anatomy*2012: Lippincott Williams & Wilkins.
4. P.Bradna, *Influence of oral cavity environment on various dental materials*. Charles University, Prague,Czech Republic, 2013.
5. Hudecki, A., G. Kiryczyński, and M.J. Łos, *Biomaterials, definition, overview*, in *Stem cells and biomaterials for regenerative medicine*2019, Elsevier. p. 85-98.
6. Gibson, L. and M. Ashby, *Cellular solids structure and properties*. Cambridge solid state science series1997, Cambridge: Cambridge University Press.
7. Boucher, E.A., *Porous materials: structure, properties and capillary phenomena*. Journal of materials Science, 1976. **11**(9): p. 1734-1750.
8. Bargmann, S., et al., *Generation of 3D representative volume elements for heterogeneous materials: A review*. Progress in Materials Science, 2018. **96**: p. 322-384.
9. Rouquerol, J., et al., *Recommendations for the characterization of porous solids (Technical Report)*. Pure and applied chemistry, 1994. **66**(8): p. 1739-1758.
10. Dullien, F.A. and V. Batra, *Determination of the structure of porous media*. Industrial & Engineering Chemistry, 1970. **62**(10): p. 25-53.
11. Cao, Y., *Representative volume element (RVE) finite-element analysis (FEA) of al metal-matrix composites*, 2016, The University of Wisconsin-Milwaukee.
12. BOUDERSSA, N., *Détermination des propriétés macroscopiques d'un matériau biphasique à microstructure aléatoire en utilisant la notion du volume élémentaire représentatif*, 2013, Université de Batna 2-Mustafa Ben Boulaid.
13. Lemaitre, S., *Modélisation des matériaux composites multiphasiques à microstructures complexes. Étude des propriétés effectives par des méthodes d'homogénéisation*, 2017, Université de CAEN Normandie.
14. Liu, L. and Z. Huang, *A note on Mori-Tanaka's method*. Acta Mechanica Solida Sinica, 2014. **27**(3): p. 234-244.
15. Barral, M., et al., *Homogenization using modified Mori-Tanaka and TFA framework for elastoplastic-viscoelastic-viscoplastic composites: Theory and numerical validation*. International Journal of Plasticity, 2020. **127**: p. 102632.
16. Bhavikatti, S., *Finite element analysis*2005: New Age International.
17. Kattan, P.I., *The Linear Triangular Element*, in *MATLAB Guide to Finite Elements*2003, Springer. p. 211-241.
18. Roylance, D., *Constitutive Equations*, 2000, Massachusetts Institute of Technology: Cambridge, MA. p. 10.
19. Barber, J.R., *Elasticity*2002: Springer.

Chapter II.

Mechanical and chemical characterization of dental materials.

Table of contents

| | |
|--|----|
| Chapter II. Mechanical and chemical characterization of dental materials. | |
| II. 1. Introduction..... | 18 |
| II. 2. Materials and methods | 19 |
| II. 3. Natural dental tissue..... | 19 |
| II. 3. 1. Natural dental tissue specimens | 20 |
| II. 3. 2. Glass-ceramic IPS d. SIGN | 22 |
| II. 3. 2. 1. IPS d. SIGN specimens..... | 23 |
| II. 4. Mechanical and chemical tests..... | 25 |
| II. 4. 1. Hardness test (Vickers)..... | 25 |
| II. 4. 2. Compressive test | 26 |
| II. 4. 3. X-ray diffraction (XRD) | 27 |
| II. 5. Results and discussion | 28 |
| II. 5. 1. Hardness test (Vickers)..... | 28 |
| II. 5. 2. Compressive test | 29 |
| II. 5. 3. X-ray diffraction (XRD) | 32 |
| II. 5. 3. 1. Natural dentin..... | 32 |
| II. 5. 3. 2. IPS d.SIGN | 33 |
| II. 6. Conclusion | 34 |
| References | 35 |

II. 1. Introduction

Glass-ceramics are used as biomaterials in various fields. Essentially, they are used as highly durable materials with a good aesthetic appearance (shape, shades of color,...) in restorative dentistry. However, teeth undergo some constraints and chemical attacks in the oral cavity that need special attention in the choice of used material as well as the manufacturing restoration process. To achieve this goal, some requirements must be fulfilled and an experimental protocol should be respected [1].

In this chapter, we are aiming to characterize the mechanical and chemical properties of the glass-ceramic IPS d.SIGN and comparing them to nature tooth mechanical and chemical properties.

II. 2. Materials and methods

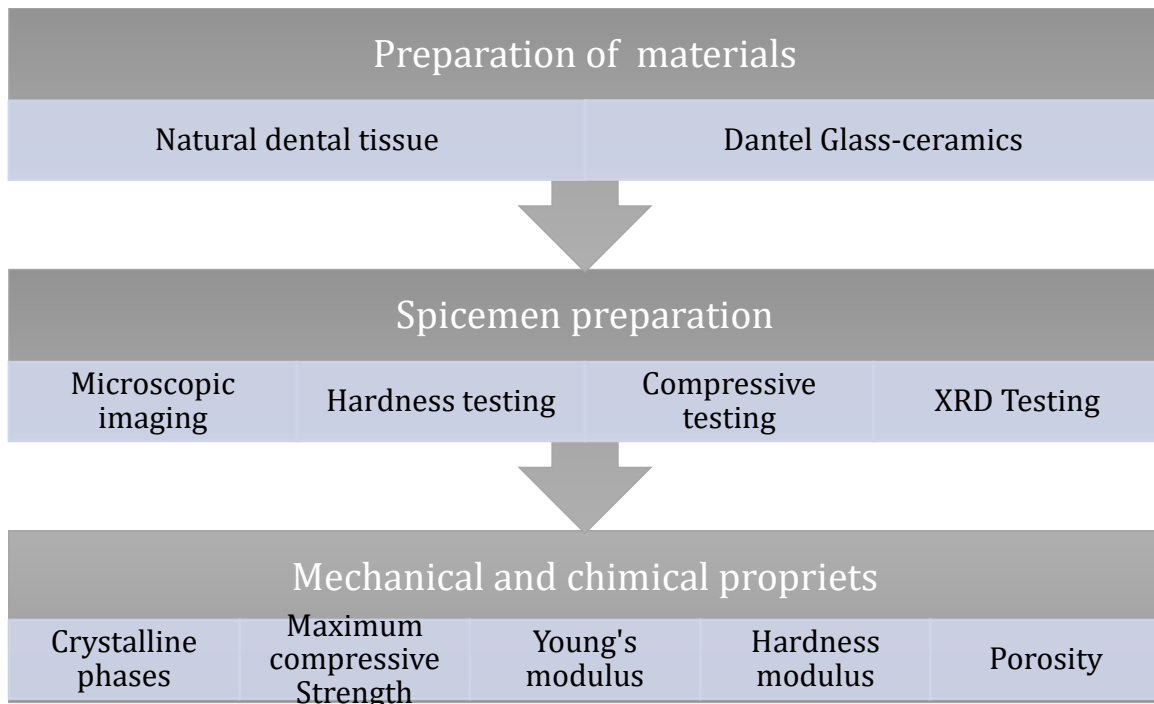


Figure II. 1.Experimental plan of work.

II. 3. Natural dental tissue

To investigate the mechanical properties of the natural dental tissue two tests were planned a hardness test and a compressive test. The teeth for these tests were obtained from adult humans and were grinded to the desired geometry and dimensions using hand tools.

According to Saint-Jean et al.[2], the natural teeth chemical formula is $\text{Ca}_5(\text{PO}_4)_3\text{OH}$ (hydroxyapatite) varying from 90% in the enamel and 70% in the dentin.



Figure II. 2. Crop view of natural tooth shows different layers.

II. 3. 1. Natural dental tissue specimens

For hardness testing, we chose a total of four specimens each one representing different zone in the tooth, to have general view of the hardness behavior of the natural tooth. **Table II. 1** illustrates the specimen's volume and density as well as the zones that were obtained from, The hardness behavior of the natural tooth is analyzed through different zones **Figure II. 3**. One specimen for enamel and three ones in dentine **Figure II. 4 (B)**.

Table II. 1.Hardness test specimens' details.

| | Size | Density (g/cm ³) | Zones |
|-----------|------------------------------------|------------------------------|-------------------|
| S1 | -- | -- | A (enamel) |
| S2 | 0.159 (cm ³) | 2.122 | B (transversal 1) |
| S3 | 0.784 (cm ³) | 1.974 | C (transversal 2) |
| S4 | 13.95×4.45×2.55 (mm ³) | 1.957 | D (longitudinal) |
| S5 | 1.50×8.26×9.75 (mm ³) | 2.448 | IPS d.SIGN. |

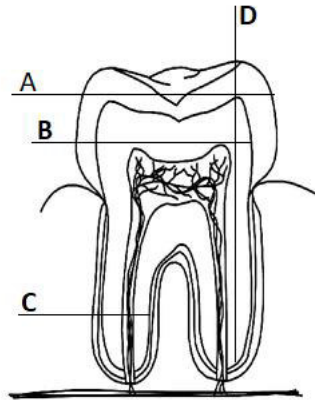


Figure II. 3.Demonstration of the zone where the specimens are taken.

For the compressive testing, we made cuboid-shaped specimens (**Figure II. 4 (A)**) from the dentin with dimensions detailed in **Table II. 2**.

Table II. 2. Compressive test specimen sizes (Dentin).

| | L (mm) | B (mm) | e (mm) | S (mm²) |
|-----------|---------------|---------------|---------------|---------------------------|
| R1 | 3.00 | 3.00 | 3.50 | 9.00 |
| R2 | 4.15 | 2.20 | 6.00 | 9.06 |

A)



B)

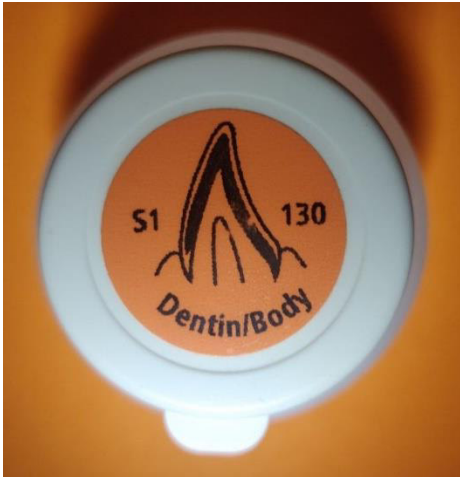


Figure II. 4. Natural dental tissue specimens for A) compressive testing and B) hardness testing.

II. 3. 2. Glass-ceramic IPS d. SIGN

The dental ceramic used in the present study is called IPS d.SIGN (fluorapatite leucite glass-ceramic). This material is developed and manufactured by the company Ivoclar Vivadent taking in account similar the natural teeth appearance and physical properties[3].

A)



B)



Figure II. 5 IPS d.SIGN A) original flask B) raw powder.

According to the manufacturer handbook [3] IPS d. SIGN glass-ceramic is consisting of:

- SiO_2 : 50–65 wt.% .
- Additional contents of Al_2O_3 , K_2O , Na_2O , CaO , P_2O_5 , F, Li_2O , ZrO_2 .
- Pigments.

IPS d.SIGN is furnished in form of fine pink powder **Figure II. 5** with average grains size of less than $50 \mu\text{m}$ **Figure II. 6**.

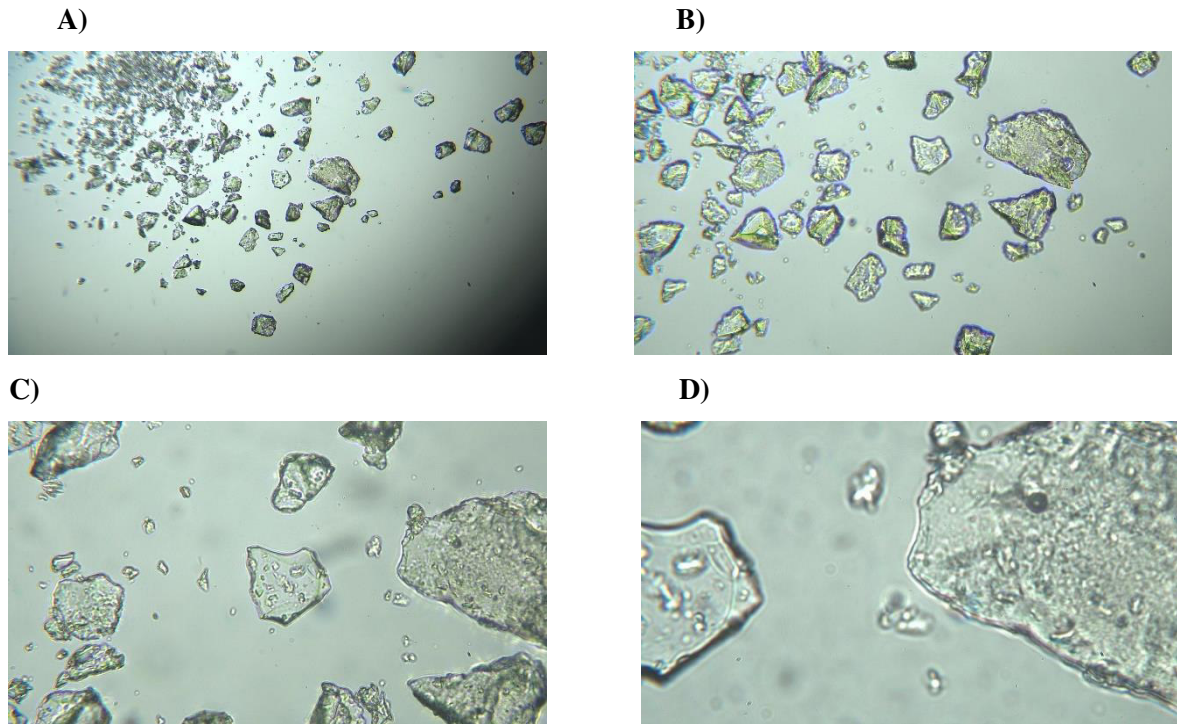


Figure II. 6. Microscopic imaging of IPS d.SIGN powder A) $\times 10$ B) $\times 20$ C) $\times 40$ D) $\times 100$.

II. 3. 2. 1. IPS d. SIGN specimens

II. 3. 2. 1. 1. Method of preparation

IPS d.SIGN glass-ceramics powder is mixed with a molding liquid (IPS d.SIGN Build-Up Liquid) until a soft paste is formed. We poured it into a cylindrical mold and stack it to avoid air bubbles. Then it is placed in a special oven (Programat P310) for 25 minutes in a specific heat cycle:

- Pre-heating: in a temperature ramp of $30\text{C}^\circ/\text{min}$.
- Maintaining: for 2min at 870C° .
- Cooling: for 4 min inside the oven (until $\sim 500\text{C}^\circ$) then continued outside the oven (ambient temperature))

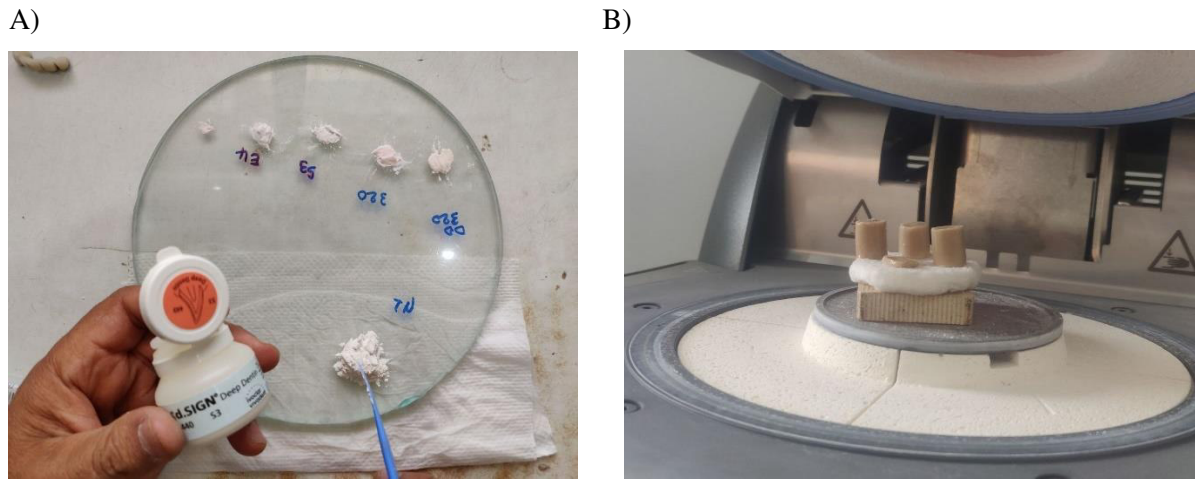


Figure II. 7.Method of preparation(A) and string(B) of IPS d.SIGN.

For hardness testing, we chose plate specimens whose dimensions are presented in **Table II. 1**, in another hand for the compressive testing we choose cylindrical shaped specimens with dimensions shown in **Table II. 3**Error! Reference source not found.. The final form of the specimens is shown in **Figure II. 8**.

Table II. 3. Compressive test specimen IPS d.SIGN sizes.

| | D (mm) | S (mm ²) | H (mm) |
|----|--------|----------------------|--------|
| C2 | 8.21 | 52.93 | 11.5 |
| C3 | 8.40 | 55.41 | 10 |

A)



B)



Figure II. 8. IPS d.SIGN specimens for A) compressive testing B) hardness testing.

II. 4. Mechanical and chemical tests

II. 4. 1. Hardness test (Vickers)

Vickers hardness test aims to determine the hardness of the material by measuring the penetration of special indenter in the concerned material. In our case, a pyramid shape with a square base and 136° between opposite faces is used (**Figure II. 9**). Load of 2 kgf is applied for 10 seconds. After indentation is made, the average of two diagonal values will be measured using a microscope, according to the following expression [4]:

$$HV = \frac{2F \sin\left(\frac{136^\circ}{2}\right)}{d^2} \quad HV = 1.854 \frac{F}{d^2} \text{ approximately} \quad \text{II. 1}$$

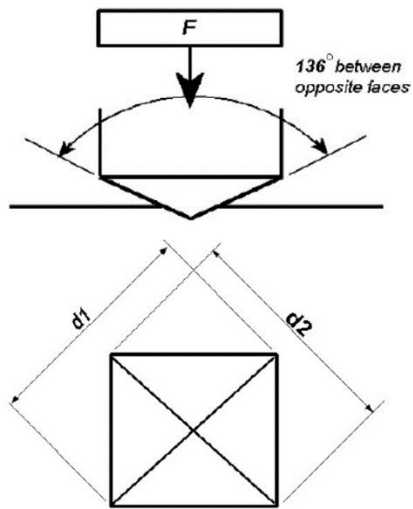
F =load in kgf..

d = the mean of the two diagonals in mm.

HV=Vickers hardness.

Vickers hardness is calculated by dividing the applied load by the area of the indentation equation **II. 1** ($HV=kgf.mm^{-2}$) [$1HV \sim 10MPa$].

A)



B)



Figure II. 9. A) indentation shape of Vickers hardness test B) Hardness testing machine (INNOVATEST).

II. 4. 2. Compressive test

The compressive test was carried out using the test machine Instron 5969 model universal machine with 50 kN load cell. **Figure II. 10 A and B.** All specimens are tested with a strain speed of 0.05 mm/mm/min. The raw data from the machine consists of load, displacement, and strain.

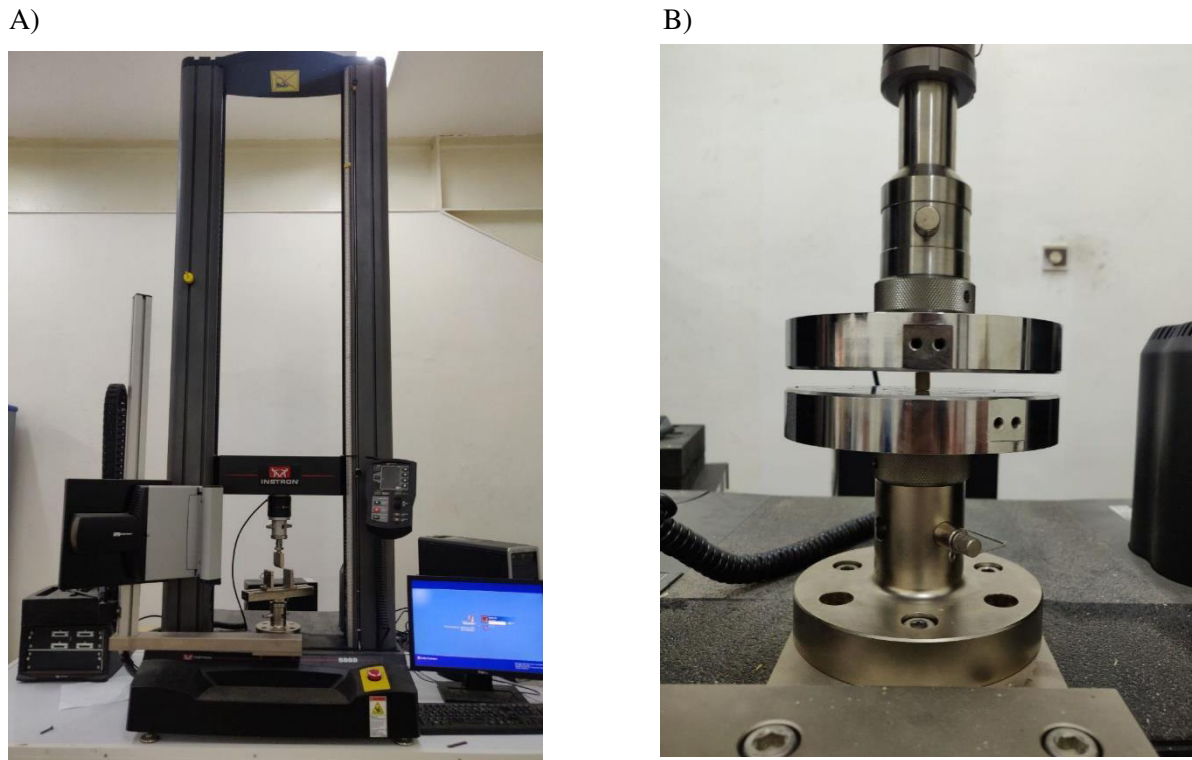


Figure II. 10. A) Compressive test machine Instron 5969, B) Specimen under compressive forces.

II. 4. 3. X-ray diffraction (XRD)

X-ray diffraction was used to access qualitative and quantitative information on the different phases formed. The crystalline structure as well, as well as the evaluation of the lattice parameters of the phases, such information easily how accessible by this method.

X-ray diffractogram patterns were performed for natural dentin and IPS d.SIGN (powder and solid) at room temperature (25°C). XRD scanning was carried out using the Cu-K emission, generating a current of 15mA, 30kV, a wavelength equal to 1.541874Å, and a continuous scanning interval of 2θ (10°–90°).

The XRD patterns were compared with International Centre for Diffraction Data (ICDD) to identify the type of crystal and crystalline phase of ceramic materials.

II. 5. Results and discussion

II. 5. 1. Hardness test (Vickers)

The mean results of the hardness tests for different regions from natural tooth (S1, S2, S3) and IPS d.SIGN (S5), **Table II. 4** . (**Figure II. 3**). Further results concerning linear path defined between B and C regions are illustrated in **Figure II. 11**.

Table II. 4.Vickers hardness test results.

| | D1 (mm) | D2 (mm) | Vickers hardness (HVN) | |
|----|---------|---------|------------------------|-----------------|
| S1 | 0.1066 | 0.1073 | 324.04 ± 4.30 | 266.10(15.9) * |
| S2 | 0.2294 | 0.2270 | 71.343 ± 1.99 | 46.30(1.7) * |
| S3 | 0.3348 | 0.3304 | 33.63 ± 0.82 | |
| S5 | 0.0681 | 0.06774 | 806.45 ±16.86 | 733.78±15.75 ** |

*data was obtained from[5].

** IPS e.max data was obtained from[6].

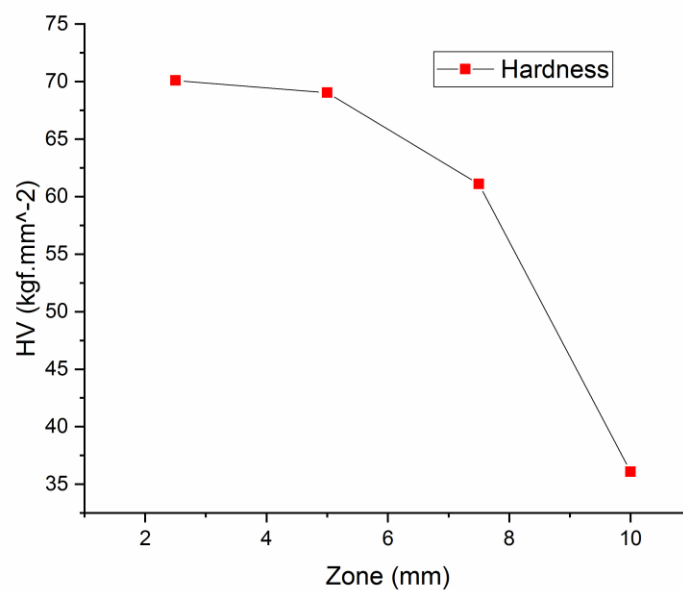


Figure II. 11.Vickers hardness test results on dentin specimen S4.

For the natural teeth, we find the average value for dentine is 52.48 HV/2 which is 11% higher than the results obtained by Wongkhantee et al.[5] . However, in enamel region, we

have noted a higher value of 17 % compared with the same work This low contrast can be explained by the fact that some mechanical properties are influenced by the degree of maturity and the age of the tooth, on one hand, and of the nature and the environmental conditions which affect it in the oral cavity, on the other hand.

We can easily notice the large deference of 6 timers higher between the enamel and the dentin hardness This difference is due to the microscopic structure of each component and the deviation of the porosity rate between them (~20%).

We also notice a strange drop in dentin hardness cross zones (high at the crown zone and low at the root). This is likely due to the density of microstructure and the concentration of the micro vine cavities (void). This parameter is also confirm by Lin et el. [7]in their work on the subject.

Using different materials which are derived from the same family of di-silicate de Lithium glass-ceramic, further comparison have been carried out with the work of Hamid et al. .[6] based on IPS e.max and the present material (IPS d.SIGN). the obtained results are reported in **Table II. 4** and reflect a good agreement with deviation of 9%.

II. 5. 2. Compressive test

The compressive test was carried out on both IPS d.SIGN and natural teeth specimens and the results are shown in the **Figure II .12 and 13** in and summered in the **Table II. 5**.

Table II. 5.Mechanical properties obtained from the compressive testing.

| | | Young's Modulus (GPa) | Maximum compressive strength (MPa) | Maximum strain (%) |
|--------------|----------------|--------------------------|--|-----------------------|
| IPS d.SIGN | C2 | 81.18 | 147.64 | 0.186 |
| | C3 | 55.75 | 96.61 | 0.153 |
| | average | 68.46 | 122.13 | 0.169 |
| IPS e.max* | CAD and PRESS | 83.5 and 82.3 | -- | -- |
| Human dentin | R1 | 17.39 | 32.49 | 0.194 |
| | R2 | 18.96 | 57.04 | 0.276 |
| | dentin average | 18.18 | 44.76 | 0.235 |
| | Human dentin | 18.60* | -- | -- |

*data obtained from[8]

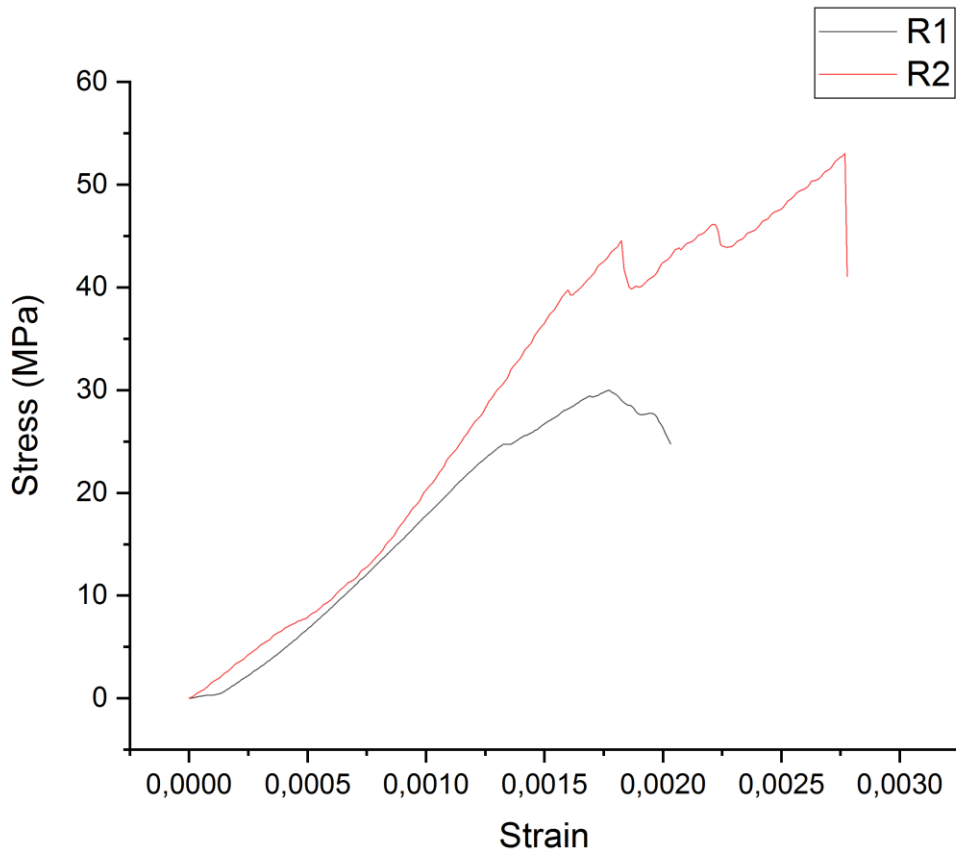


Figure II. 12. Stress-strain curve of compressive test on natural Dentin.

Compressive strength results for natural dentine are presented in **Figure II. 12**Figure II. 12. Two different regions can be noted in both curves. Firstly, an elastic part is presented with a linear slope of 18.3 GPa. This value concerning Young's modulus is similar and almost identical to that reported by Flavia et al. [8]. Secondly, disturbed curves are depicted with disturbed piecewise linear parts. This can be explained by the heterogeneous of the dental composition material and the complexity of the microstructure.

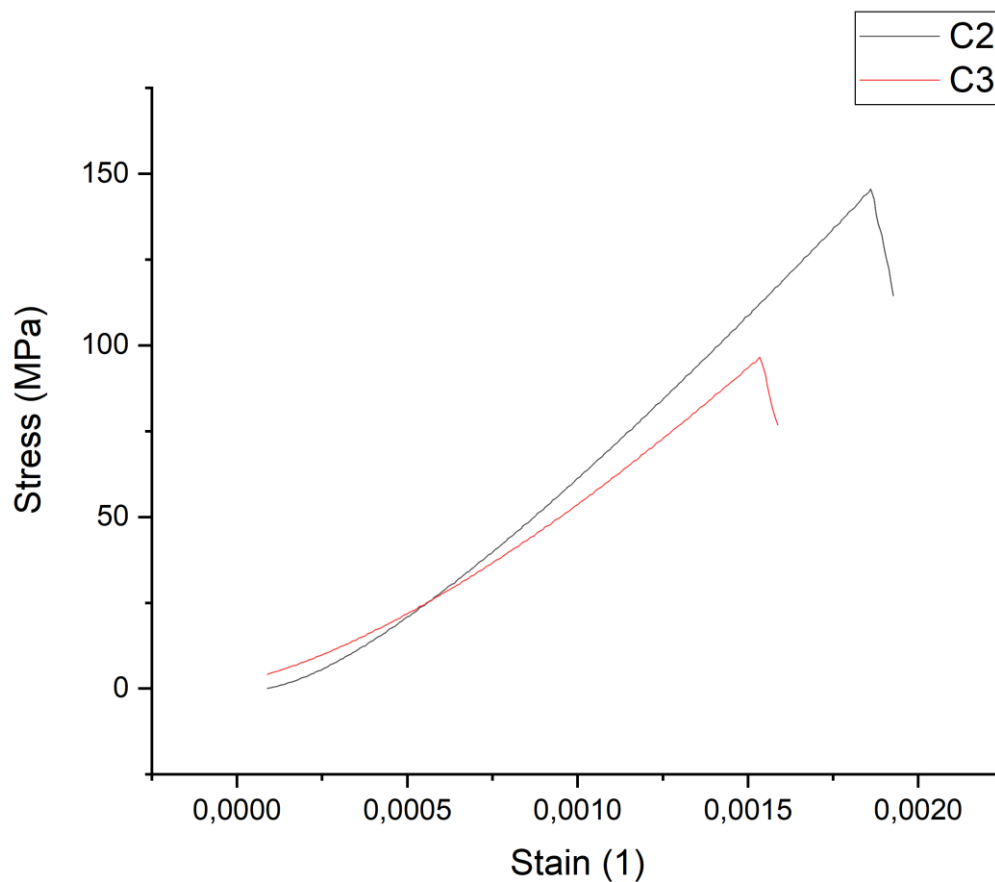


Figure II. 13. Stress-strain curve of compressive test on IPS d.SIGN.

The results of the compressive test for IPS d.SIGN is shown in **Figure II. 13**, we can notice a linear elastic damageable behavior revealing a brittle material (the absence of the plastic region). The obtained Young's modulus is about 68 GPa. When it is compared to those assessed by Flavia et al. [8] for respectively IP e.max CAD and PRESS, average deviations are 21% and 20%.

II. 5. 3. X-ray diffraction (XRD)

II. 5. 3. 1. Natural dentin

The XRD results are shown in Figure II. 14, narrow diffraction peaks which confirm the presences of compounds of similar intensity. The diffraction peaks detected in the XRD patterns are characteristic of calcium Hydrogen phosphate hydroxide (ICCD 046-0905).

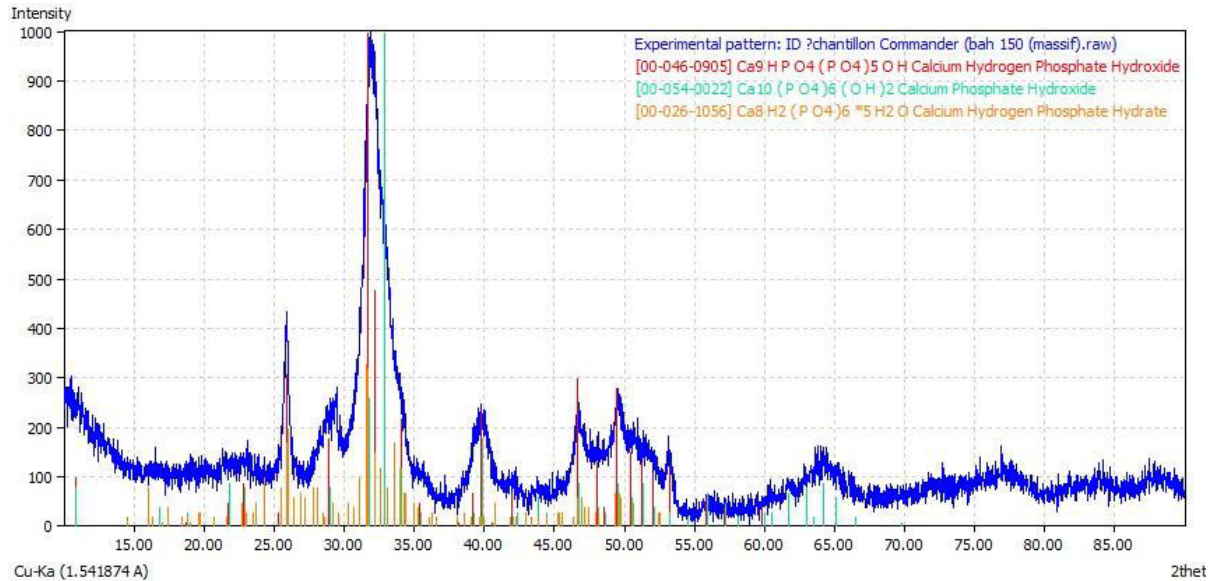


Figure II. 14. XRD curve results for natural dentin.

II. 5. 3. 2. IPS d.SIGN

The XRD results for IPS d.SIGN are shown in **Figure II. 15** and **Figure II. 16**.

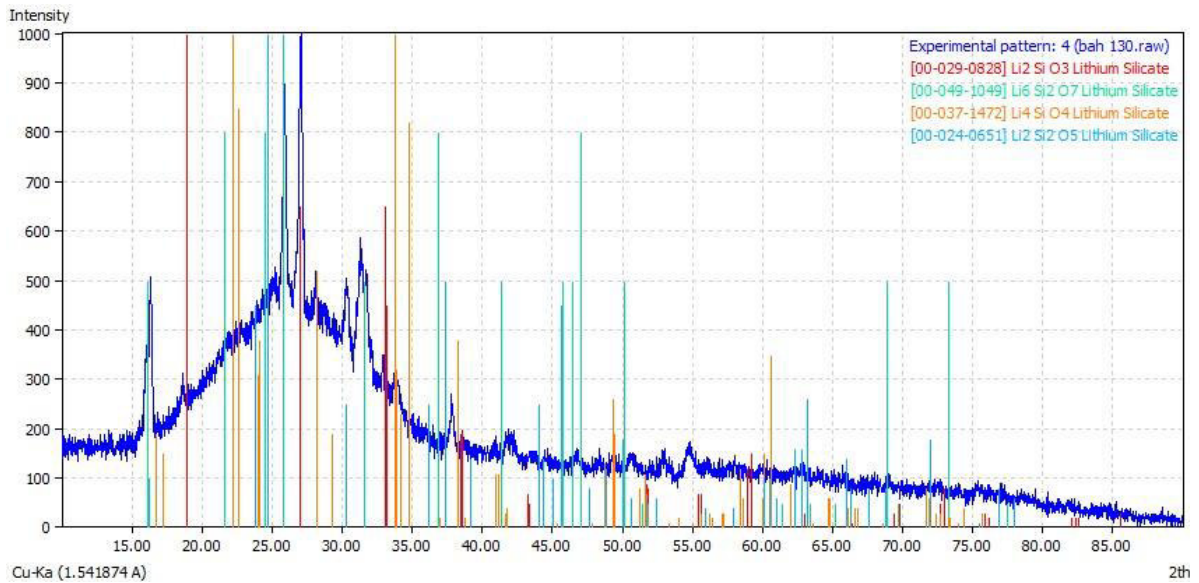


Figure II. 15. XRD curve results for IPS d.SIGN powder.

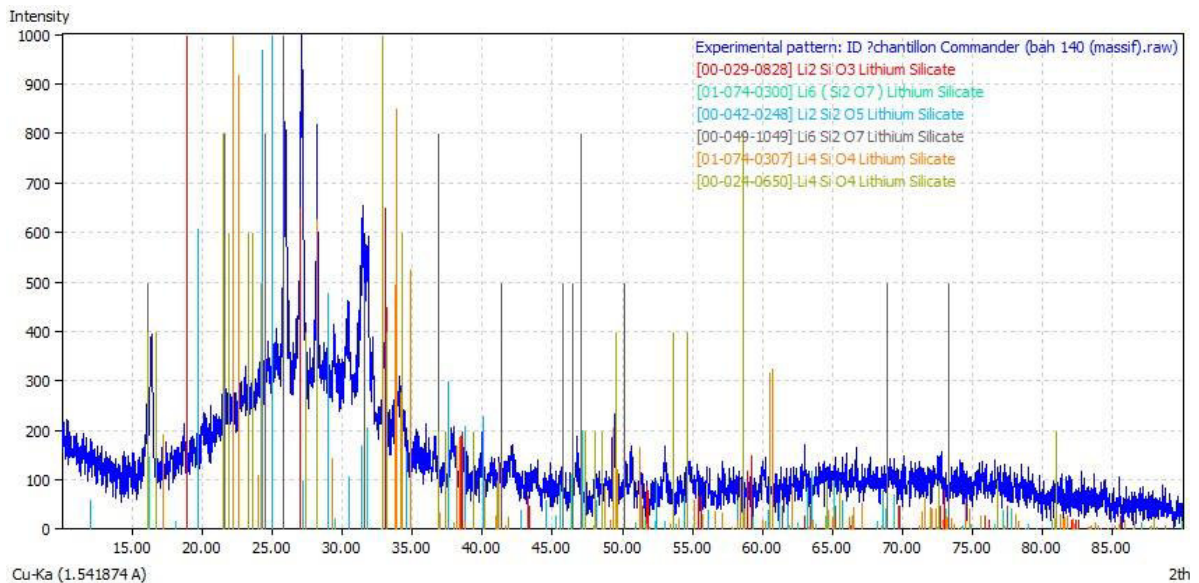


Figure II. 16. XRD curve results for IPS d.SIGN solid.

Both ceramics presented comparable, narrow diffraction peaks, which confirm the formation of crystalline compounds of similar intensity. The dome shape and smooth curve reveals an amorphous glass phase. In addition, the diffraction peaks detected in XRD patterns are characteristic of Lithium Silicate (ICCD 029-0828 crystals, that confirms the presence of crystalline compounds for IPS d.SIGN).

II. 6. Conclusion

experimental work was carried out in this part of the thesis and which consists of mechanical characterization and chemical analysis of the IPS d.SIGN material (glass-ceramic) and the natural tooth. Compression tests and hardness measurement are carried out on the different types of materials. Chemical analysis is limited to the definition of crystalline phases using x-Ray diffraction (XDR).

The obtained results can be summarized as following:

- The hardness of synthetic glass-ceramic is three times greater than the enamel one. However, the hardness of the dentine material presents lower value, estimated around one sixth of the one of enamel.
- From the compression test carried out on the materials tested in this work, the results obtained confirm that the Young's modulus and the compressive stress of the IPS d.SIGN material are three times greater than those of natural dentine.
- For the XRD testing for both materials, natural dentine and IPS d.SIGN glass-ceramic confirms the presents of crystalline phase as hydroxyapatite and lithium silicate ,respectively.

References

1. Höland, W., et al., *Clinical applications of glass-ceramics in dentistry*. Journal of Materials Science: Materials in Medicine, 2006. **17**(11): p. 1037-1042.
2. Saint-Jean, S.J., *Dental glasses and glass-ceramics*, in *Advanced ceramics for dentistry*2014, Elsevier. p. 255-277.
3. Vivadent, I., *IPS d.SIGN Instructions for Use*, 2008: Liechtenstein. p. 68.
4. Herrmann, K., *Hardness testing: principles and applications*2011: ASM international.
5. Wongkhantee, S., et al., *Effect of acidic food and drinks on surface hardness of enamel, dentine, and tooth-coloured filling materials*. Journal of dentistry, 2006. **34**(3): p. 214-220.
6. Kermanshah, H., et al., *Vickers micro-hardness study of the effect of fluoride mouthwash on two types of CAD/CAM ceramic materials erosion*. BMC Oral Health, 2022. **22**(1): p. 1-8.
7. Lin, Y.-S., *Bio-inspired tailored hydroxyapatite-based powder composites for dental applications*, 2012, UC San Diego.
8. Trindade, F.Z., et al., *Elastic properties of lithium disilicate versus feldspathic inlays: effect on the bonding by 3D finite element analysis*. Journal of Prosthodontics, 2018. **27**(8): p. 741-747.

Chapter III.

Numerical modeling of the thermo-elastic behavior of porous materials.

Table of Contents

| | |
|--|----|
| Chapter III. Numerical modeling of the thermo-elastic behavior of porous materials. | |
| III. 1. Introduction | 37 |
| III. 2. The thermo-elastic behavior of non-porous glass-ceramic: | 37 |
| III. 3. Effective Young's modulus and Poisson's ratio of Air: | 38 |
| III. 3.1. Numerical Approach FEA: | 39 |
| III. 3.2. Analytical Approach Mori-Tanaka | 39 |
| III. 4. Multiscale Modeling and Homogenization of porous ceramics | 39 |
| III. 5. Results and discussion | 41 |
| III. 5.1. The thermo-elastic behavior of non-porous glass-ceramic: | 41 |
| III. 5.2. Effective Young's modulus and Poisson's ratio of air:..... | 42 |
| III. 5.3. Multiscale Modeling and Homogenization of porous ceramics | 44 |
| III. 6. Conclusion | 47 |
| References | 48 |

III. 1. Introduction

In this chapter, we aim to model the thermo-elastic behavior of porous dental restorative materials. In addition to the IPS d.SIGN analyzed in previous experimental work, the IPS e.max CAD is also introduced in numerical simulations as material constituting of porous microstructures. To achieve this purpose, firstly, the glass-ceramics are considered as multi-phases composites without pores where the matrix phase is SiO_2 .

This approach is based on the amount and thermo-mechanical properties of chemical constituents already known. After that, the pores are assumed as elastic infinitesimal solid with adequate properties. The obtained values will be used in second step for modeling the real porous glass-ceramics. Both analytical model (Mori-Tanaka) and numerical method (Finite Element Method) will be used to assess the homogeneous thermo-mechanical properties of the porous IPS e.max CAD and IPS d.SIGN.

III. 2. The thermo-elastic behavior of non-porous glass-ceramic:

In order to assess the non-porous thermal and mechanical elastic properties of IPS e.max CAD glass-ceramic, an analytical homogeneous analysis is performed using Mori-Tanaka mean field approach. We consider the heterogeneous material whose microstructure consists of SiO_2 as a matrix material and multiple phases of so-called

“inclusions”. According to the analysis achieved by Švančárková et al. [1], chemical and mechanical data properties of different components are reported in **Table III. 1**

Table III. 1. IPS e.max CAD composition, mechanical and physical properties.

| Composition | IPS e.max CAD (w%) [1] | E (GPa) | NU | Density (g/cm ³) | Thermal Expansion (1E-6/K°) |
|--|---------------------------|-----------|-----------|---------------------------------|-----------------------------------|
| SiO ₂ ^[2] | 67.5* | 66.3-74.8 | 0.15-0.19 | 2.17-2.65 | 0.55-0.75 |
| Li ₂ O ^[3] | 14.3 ± 0.8 | 140 | 0.2 | 2.013 | 25.91 |
| Al ₂ O ₃ ^[4] | 4.8 ± 0.1 | 215-413 | 0.21-0.33 | 3-3.98 | 4.5-10.9 |
| P ₂ O ₅ ^[5-7] | 4.3 ± 0.2 | 30.7 | 0.26 | 2.52 | 10.58 |
| K ₂ O ^[8, 9] | 9.1 ± 1.3 | 67.11 | 0.1651 | 2.35 | 13-26 |
| Na ₂ O ^[10, 11] | ----- | 93.2 | 0.223 | 2.27 | 9.59 |

*Summed to 100

We use the same homogeneous approach to analyses the IPS d.SIGN thermo-elastic behavior. However, the same component properties are used with mass fractions reported in the work of Kukiattrakoon et al. [12], data are illustrated on **Table III. 2**.

Table III. 2. Composition of IPS d.SIGN in (w%).

| Composition | IPS d.SGIN (w%)[12] |
|--------------------------------|---------------------|
| SiO ₂ | 65 |
| Na ₂ O | 8 |
| Al ₂ O ₃ | 0.25 |
| P ₂ O ₅ | 16.75 |
| K ₂ O | 10 |

III. 3. Effective Young's modulus and Poisson's ratio of Air:

To evaluate the effective elastic properties of the air, two parametric analysis approaches of micro-structural homogenization based on porous titanium were carried out Mori-Tanaka Approach (M.T.A) and Finite Element Method (F.E.M). Two hypotheses are considered herein, firstly it is assumed that the microstructure is a homogeneous medium with voids (cavities), and secondly it is considered as a porous material, by assigning the properties of air to the porous areas.

III. 3.1. Numerical Approach FEA:

A numerical FEM analysis is performed to study a Titanium scaffolds elastic behavior, used in bones implantation, reported by Torres et al. [13]. An open-source MATLAB code is applied to generate a microstructure of porous medium.

The generated microstructural consists of an RSE size of 1 mm^2 , porosity of 0.55, and a pores size of $120 \text{ }\mu\text{m}$ with the random distribution **Figure III. 1 (a)**. The RSE was exported to COMSOL Multiphysics.

The simulation was executed in two parts. First, the porous was treated as void and was subtracted from the geometry of RSE **Figure III. 1 b)**. Second the porous was treated as a phase **Figure III. 1 c)**, and it was given Young's modulus between 1 to $1\text{E}+9$ (Pa) and Poisson's ratio of 0 to 0.5.

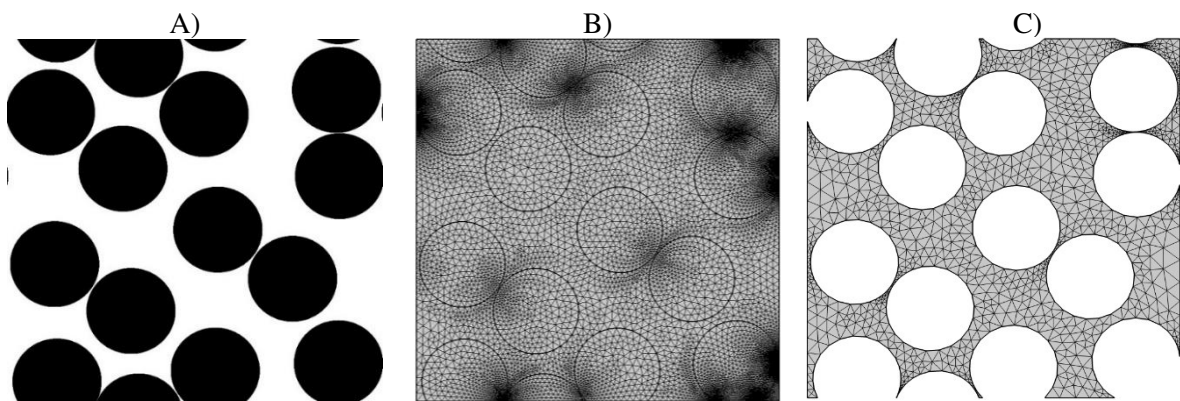


Figure III. 1. A) RSE generated by MATLAB B) inclusion phase treated as void C) inclusion phase treated as air.

III. 3.2. Analytical Approach Mori-Tanaka

The Digmat MF (Mean Field Homogenization tool) is used to reach an acceptable level of similarity between the air and the void effects on the global properties on the homogeneous microstructure. This is achieved by the same parametric analysis already done in the FEM section.

III. 4. Multiscale Modeling and Homogenization of porous ceramics

Based on the work reported in Lucas et al. [14], a microstructure of IPS e.max CAD is adopted to compute the homogenization macro-mechanical elastic properties. The image obtained by the micro-CT scan technology, **Figure III. 2 a)** is used to build the RSE. The presence of porous area can be noticed by dark bubbles. The image is binarized using a

Graphic processing software (GIMP 2.0, **Figure III. 2 b**). On the other hand, a second microscopic image of IPS d.SIGN has been processed to evaluate effect of porosity on thermo-elastic behavior of another kind of ceramic, **Figure III. 3 b**) and **Figure III. 3 b**). It should be noticed that both materials (IPS e.max CAD and IPS d.SIGN) have close porosities (0.1547 and 0.1537), respectively.

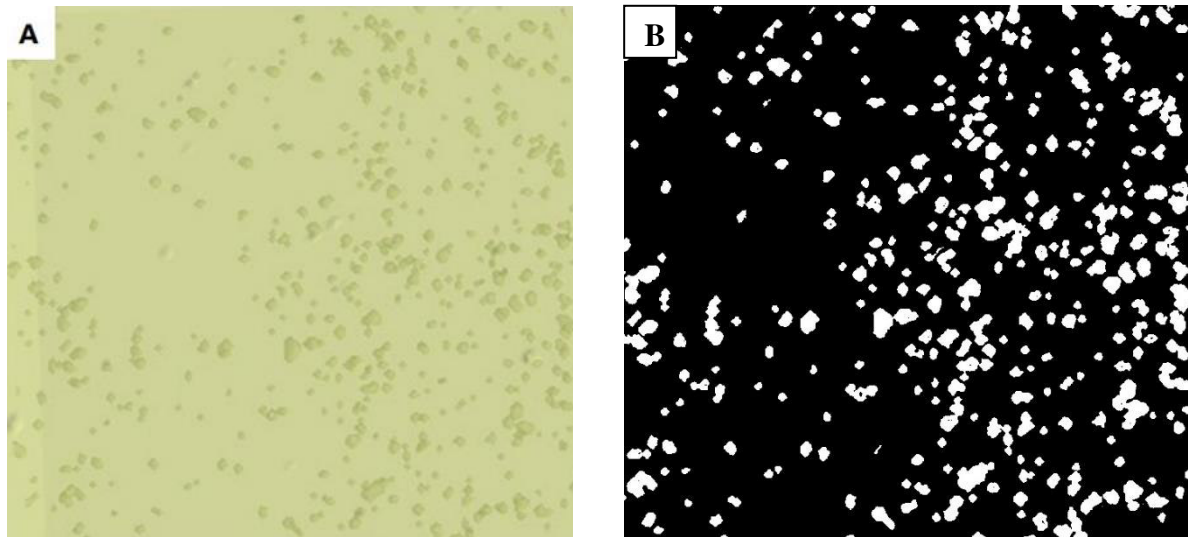


Figure III. 2.The RSE of IPS e.max CAD (A) raw micro-CT scan picture (B) treated picture (binarized).

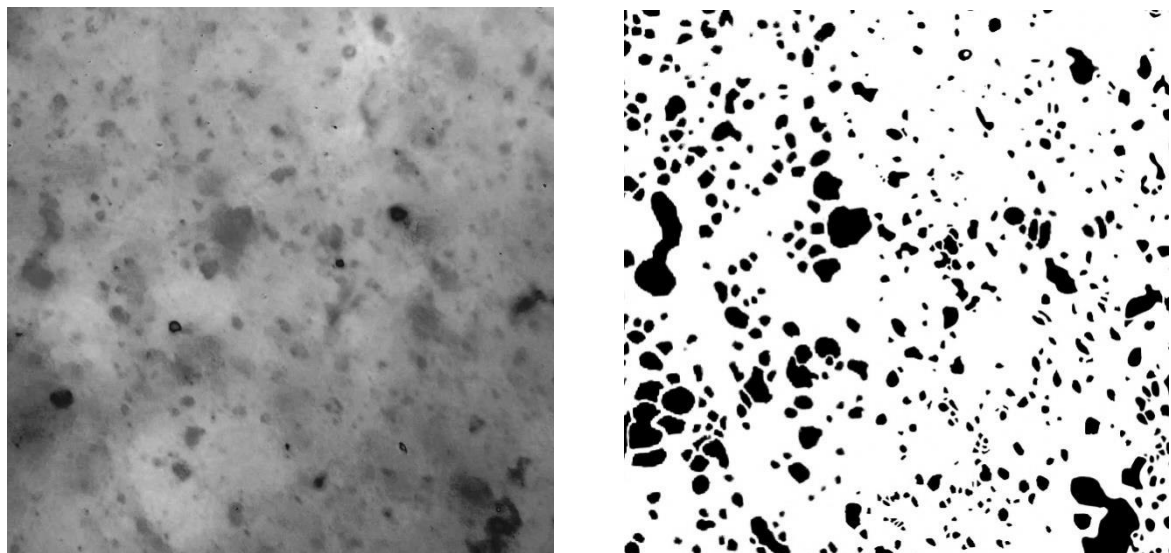


Figure III. 3. IPS d.SIGN microscopic images size of A) raw B) binarized.

Both materials are considered as biphasic porous structures; pores phase and glass-ceramic phase. It is assumed that the pore has a linear elastic behaviour with a very low Young's modulus of 1 Pa and Poisson's ratio equal to 0. The elastic thermo-elastic

$$\begin{array}{c}
 \text{Thermal expansion (1/K}^\circ\text{)} \qquad \qquad \qquad 7.33\text{E-}006 \qquad \qquad \qquad 8.2298\text{E-}006 \\
 \hline
 C_{IPS\ d.SIGN} \\
 = \begin{bmatrix}
 9.593\text{E} + 010 & 2.1391\text{E} + 010 & 2.1391\text{E} + 010 & & & \\
 2.1391\text{E} + 010 & 9.593\text{E} + 010 & 2.1391\text{E} + 010 & & & 0 \\
 2.1391\text{E} + 010 & 2.1391\text{E} + 010 & 9.593\text{E} + 010 & & & \\
 & & & 3.727\text{E} + 010 & & 0 \\
 & 0 & & 0 & 3.727\text{E} + 010 & 0 \\
 & & & 0 & 0 & 3.727\text{E} + 010
 \end{bmatrix} \\
 \\
 \alpha_{IPS\ d.SIGN} = \begin{bmatrix}
 6.8849\text{E} - 006 & & 0 & & 0 \\
 & 0 & & 6.8849\text{E} - 006 & & \\
 & & 0 & & 0 & \\
 & & & 0 & & 6.8849\text{E} - 006
 \end{bmatrix} \qquad \qquad \qquad \text{III.2}
 \end{array}$$

Table III. 4. The thermal and mechanical proprieties of non-porous IPS d.SIGN.

| | Low of mixtures | Mori-Tanaka |
|--------------------------|-----------------|-------------|
| Young's Modulus (Pa) | 9.031E+010 | 8.8129E+010 |
| Poison's ratio (1) | 0.18 | 0.1823 |
| Thermal expansion (1/K°) | 7.76E-006 | 6.8849E-006 |

We note that all results for both glass-ceramics are very close, where Young's modulus are around 88 and 85 GPa. However, a similar Poison's ratio of 0.18 is obtained for the two glass-ceramic materials. In contrast, some difference of homogeneous thermal expansion coefficient is found. The previous results can be explained by the property value of the dominant phase in each material.

III. 5.2. Effective Young's modulus and Poisson's ratio of air:

Figure III. 4 shows the effect of the Poison's ratio of air on Poison's ratio of air of porous Titanium. using only the Mori-Tanaka method. It seems that the Poisson ratio is not affected to that of Air.

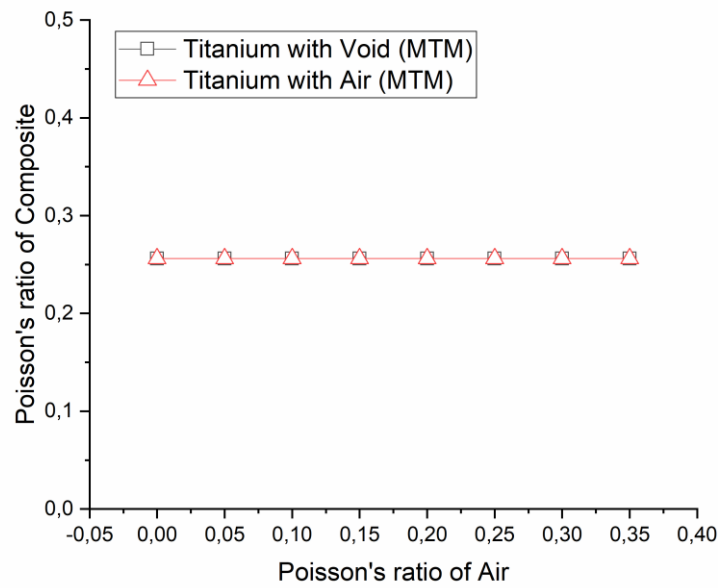


Figure III. 4. The effect of the Poisson's ratio of air on Poisson's ratio of air of porous Titanium.

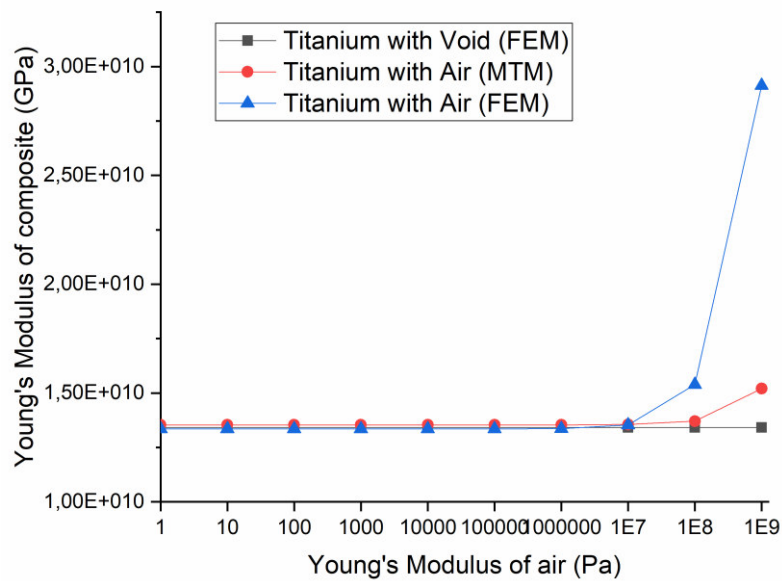


Figure III. 5. The effect of the elastic property of air on Young's modulus of porous Titanium.

Figure III. 5 shows the effect of the elastic property of air on Young's modulus of porous Titanium. Since the Young's modulus of the air is under 10 MPa, invariant results of the Young's modulus of the Titanium, equal to 13.4 GPa is obtained. A value that is in a good agreement with that obtained by Torres et al. [13].

III. 5.3. Multiscale Modeling and Homogenization of porous ceramics

Figure III. 6 A and B shows an adaptive free mesh generated by COMSOL Multiphysics. The states of stresses are illustrated in Figure III. 7. A) and B) for both glass-ceramics IPS e.max CAD and IPS d.SIGN, respectively. And the state of strain is shown in Figure III. 8 A) and B) for the same materials.

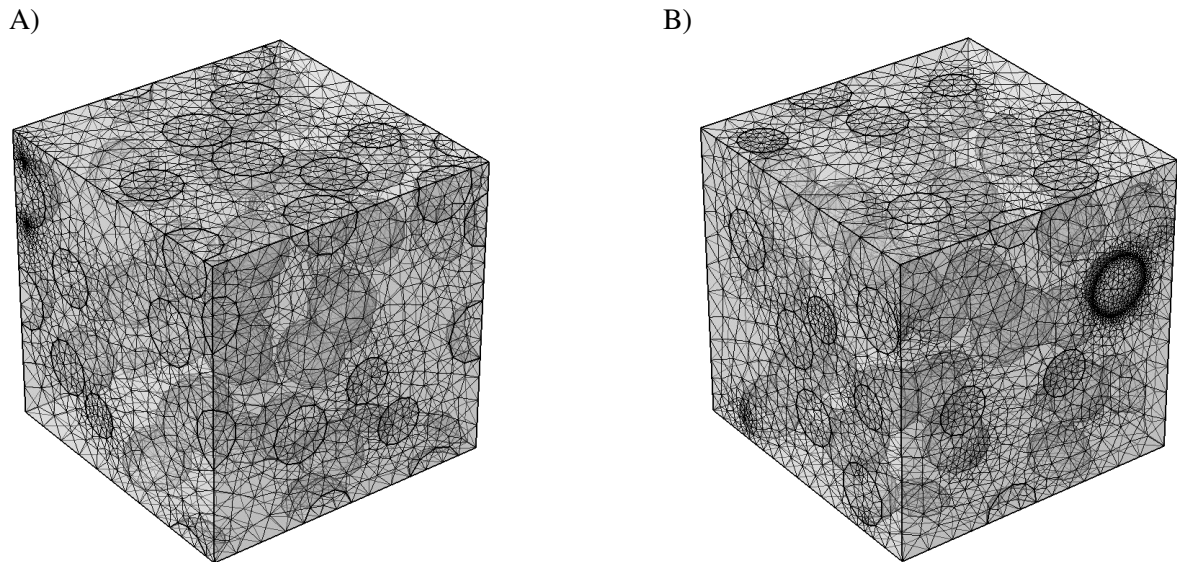


Figure III. 6. Meshed microstructure for (A) IPS e.max CAD (B) IPS d.SIGN .

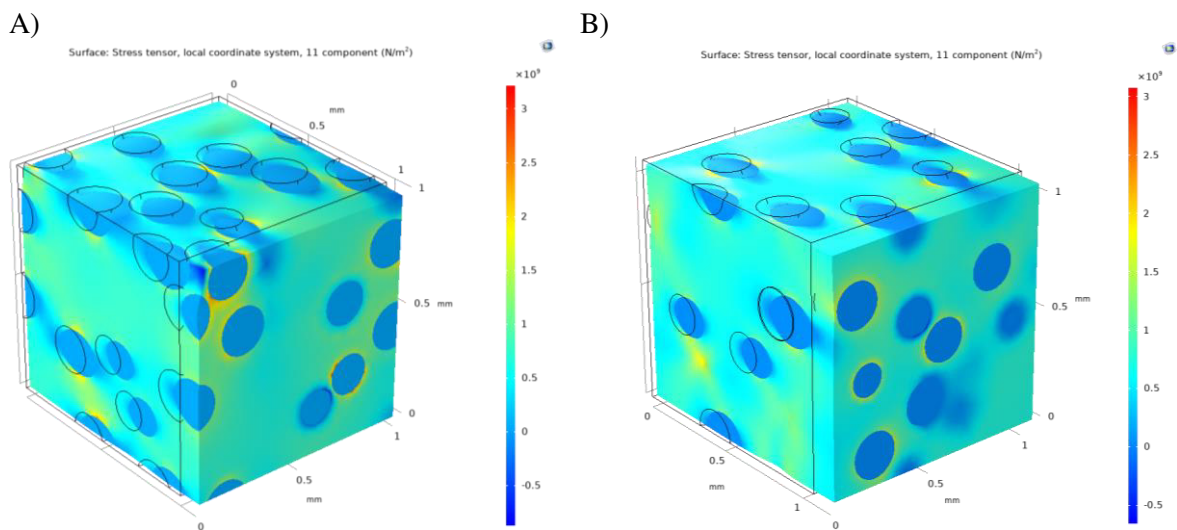


Figure III. 7. State of stress of (A) IPS e.max CAD (B) IPS d.SIGN, using COMSOL.

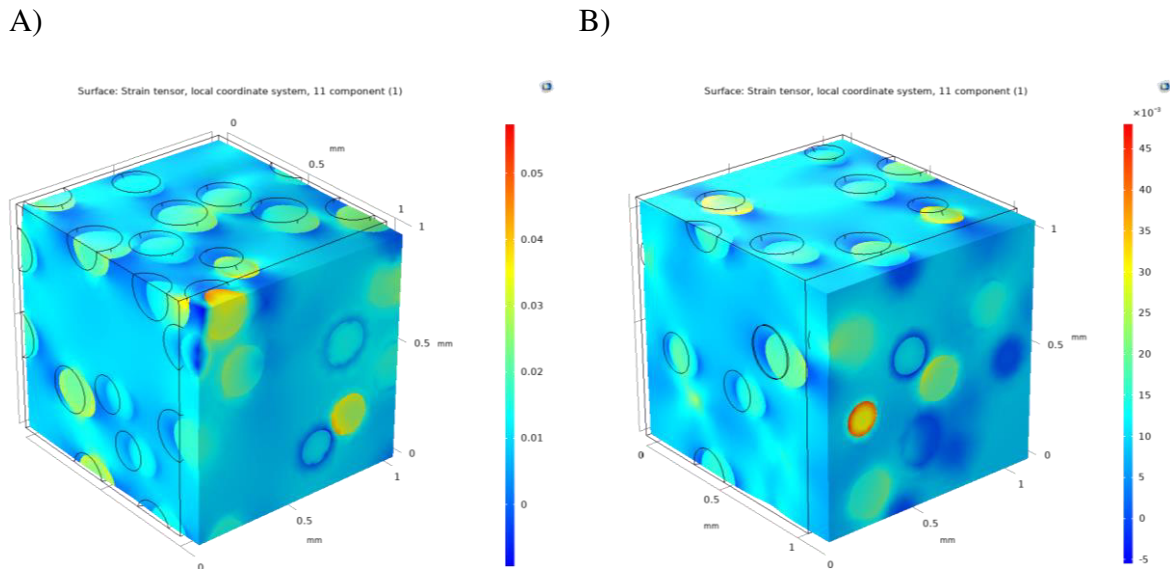


Figure III. 8. State of strain of (A) IPS e.max CAD (B) IPS d.SIGN using COMSOL.

Firstly, **Figure III. 7.** highlights stress concentrations through the transverse axis around all cavities. Phenomena in line with the hole plates theories. This is generally explained by the discontinuity of the micro-structural material. The average stress and strain tensor components are obtained in post-processor of COMSOL analysis, **Table III. 5** And **Table III. 7.** Hence, the elastic properties are deduced and reported in **Table III. 6** and **Table III. 8.** Further results included in the same Table are computed using the Mori-Tanaka method and the correlation method, given by Lu et al. [15]. Results of Young's modulus for both homogeneous materials show lower values than the one of non-porous glass-ceramic. In contrast, slight increase of Poisson's ratio is observed.

Table III. 5. Average values for Stress and Strain tensors for the IPS e.max CAD RVE.

| Strain | (1) | Stress | (Pa) |
|------------|------------|------------|----------------|
| E11 | 0.0099 | S11 | 6.1748E8 |
| E12 | -5.3254E-5 | S12 | -1645932.71204 |
| E13 | -5.0532E-5 | S13 | -3592158.00808 |
| E22 | -0.0018 | S22 | 2.6064E-6 |
| E23 | 8.4262E-6 | S23 | -487723.8097 |
| E33 | -0.0017 | S33 | 2.8924E-6 |

Table III. 6.Engineering modulus of the homogenous IPS e.max CAD glass ceramic.

| | FEM COMSOL | DIGIMAT FE | DIGIMAT MF |
|----------------------|-------------|--------------|-------------|
| Young's Modulus (Pa) | 6.1748E+010 | 6.410E+010 | 6.252E+010 |
| Poison's ratio | 0.1835 | 0.1776 | 0.18311 |
| Shear Modulus (Pa) | 2.6087E+010 | 2.7216 E+010 | 2.6422E+010 |

E= 6.5130e+010 (GPa) using correlation [15]

Table III. 7. Average values for Stress and Strain tensors for the IPS d.SIGN RVE.

| Strain | (1) | Stress | (Pa) |
|------------|------------|------------|---------------|
| E11 | 0.0093 | S11 | 6.0744E8 |
| E12 | -1.3087E-6 | S12 | 137744.1634 |
| E13 | -1.7694E-5 | S13 | -1110080.1405 |
| E22 | -0.0017 | S22 | 5.3483E-6 |
| E23 | -5.1009E-6 | S23 | -187462.7852 |
| E33 | -0.0017 | S33 | 1.7799E-6 |

Table III. 8. Engineering modulus of the homogenous IPS d.SIGN glass-ceramic.

| | FEM COMSOL | DIGIMAT FE | DIGIMAT MF |
|----------------------|--------------|--------------|-------------|
| Young's Modulus (Pa) | 6.4775e+010 | 6.597e+010 | 6.4852E+010 |
| Poison's ratio | 0.1841 | 0.1801 | 0.18509 |
| Shear Modulus (Pa) | 2.7352 e+010 | 2.7951 e+010 | 2.7362E+010 |

E= 6.7242e+010(GPa) using correlation [15]

Regarding the thermo-elastic behavior analysis, where a constant thermal loading is applied, results are shown in **Figure III. 9** and **Figure III. 10** for displacement magnitude and Von-Mises stress, respectively for both materials

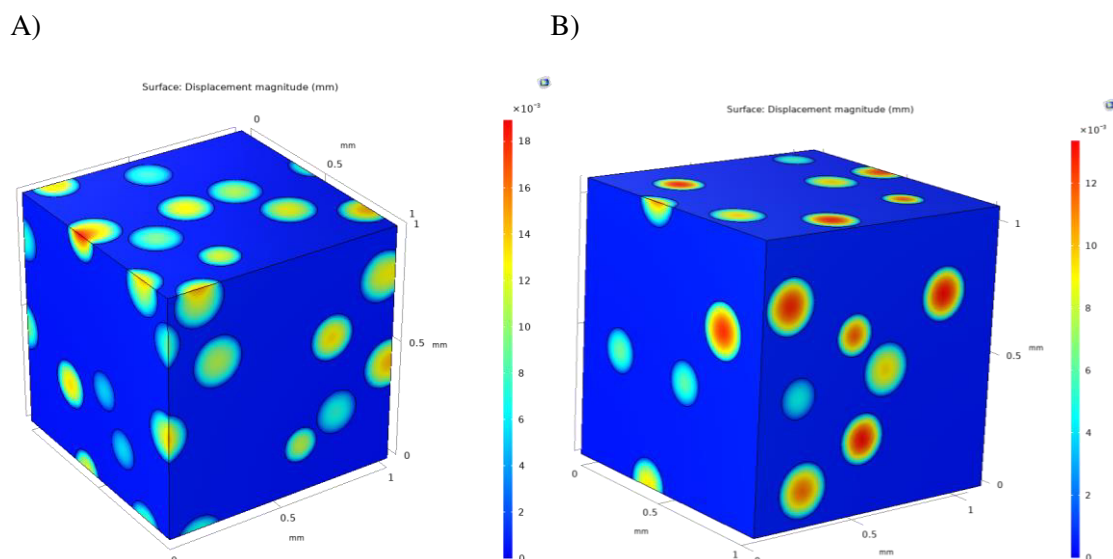


Figure III. 9. State of displacement magnitude for A) IPS e.max CAD B) IPS d.SIGN, using COMSOL.

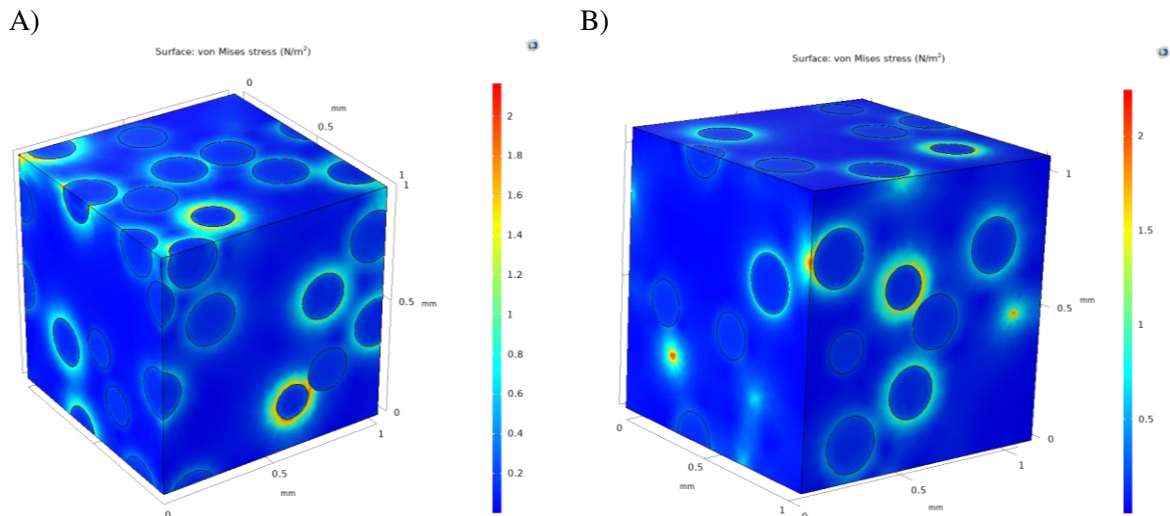


Figure III. 10. State of Von-Mises stresses for A) IPS e.max CAD B) IPS d.SIGN, using COMSOL.

We can deduce that the CTE of the porous glass-ceramics depends only upon the matrix phase properties and seems not affected by the air's thermo-elastic properties. This phenomena is in a good agreement with work of Molin et al.[16]

III. 6. Conclusion

In the present chapter, a multi-scale homogeneous approach is adopted to analysis the thermo-elastic behavior of two glass-ceramic materials.

Based on Macro-mechanical equivalent properties, analysis is focused on Young's modulus, Poisson ration and coefficient of thermal expansion. We can highlight the following conclusions:

- The pores can be modeled as an air with Young's modulus less than 10 MPa.
- Porosity decreases the elastic modulus of glass-ceramics.
- The Poisson's ration and the CTE of the global structure is not affected by any thermo-elastic properties of air exclusively for Young's modulus less the 10 MPa.

References

1. Švančárková, A., et al., *Effect of Corrosive Media on the Chemical and Mechanical Resistance of IPS e. max® CAD Based Li₂Si₂O₅ Glass-Ceramics*. *Materials*, 2022. **15**(1): p. 365.
2. Lucideon. *Silica - Silicon Dioxide (SiO₂)*. 2001 [cited Dec 13 2001; Available from: <https://www.azom.com/article.aspx?ArticleID=1114>].
3. Report, R.T.S., *The use of lithium oxide as the breeder in fusion reactors*, 1989. p. 30.
4. Lucideon. *Alumina - Aluminium Oxide - Al₂O₃ - A Refractory Ceramic Oxide*. 2001 [cited Feb 6 2001; Available from: <https://www.azom.com/article.aspx?ArticleID=52>].
5. Ainsworth, R.I., D.D. Tommaso, and N.H. de Leeuw, *A density functional theory study of structural, mechanical and electronic properties of crystalline phosphorus pentoxide*. *The Journal of chemical physics*, 2011. **135**(23): p. 234513.
6. Corti, H.R., F.J. Nores-Pondal, and C.A. Angell, *Heat capacity and glass transition in P₂O₅-H₂O solutions: support for Mishima's conjecture on solvent water at low temperature*. *Physical Chemistry Chemical Physics*, 2011. **13**(44): p. 19741-19748.
7. Guo, W., et al., *Joining high volume fraction SiC particle reinforced aluminum matrix composites (SiCp/Al) by low melting point stannous oxide-zinc oxide-phosphorus pentoxide glass*. *Ceramics International*, 2021. **47**(3): p. 3955-3963.
8. Dovesi, R., et al., *On the elastic properties of lithium, sodium and potassium oxide. An ab initio study*. *Chemical Physics*, 1991. **156**(1): p. 11-19.
9. Guder, V. and S.S. Dalgic, *Thermodynamic properties of potassium oxide (K₂O) Nanoparticles by molecular dynamics simulations*. *Acta Physica Polonica A*, 2017. **131**(3): p. 490-494.
10. Gavriľiu, G., *Thermal expansion and characteristic points of Na₂O-SiO₂ glass with added oxides*. *Journal of the European Ceramic Society*, 2002. **22**(8): p. 1375-1379.
11. Phacheerak, K. and T. Noinonmueng, *Structural and Mechanical Properties of Cubic Na₂O: First-Principles Calculations*. *Journal of Applied Research on Science and Technology (JARST)*, 2020. **19**(2): p. 17-24.
12. Kukiattrakoon, B., P. Junpoom, and C. Hengtrakool, *Vicker's microhardness and energy dispersive x-ray analysis of fluorapatite-leucite and fluorapatite ceramics cyclically immersed in acidic agents*. *Journal of Oral Science*, 2009. **51**(3): p. 443-450.
13. Torres-Sanchez, C., et al., *The effect of pore size and porosity on mechanical properties and biological response of porous titanium scaffolds*. *Materials Science and Engineering: C*, 2017. **77**: p. 219-228.
14. Tavares, L.d.N., et al., *Microstructural and mechanical analysis of two CAD-CAM lithium disilicate glass-reinforced ceramics*. *Brazilian oral research*, 2020. **34**.
15. Lu, G. and Z. Xiao, *Mechanical properties of porous materials*. *Journal of Porous Materials*, 1999. **6**(4): p. 359-368.
16. Molina, J.-M., et al., *Porosity effect on thermal properties of Al-12 wt% Si/graphite composites*. *Materials*, 2017. **10**(2): p. 177.

Chapter VI.

Numerical 3D modeling of the thermo-elastic behavior of
restorative materials.

Table of Contents

| | |
|---|----|
| Chapter IV. Numerical 3D modeling of the thermo-elastic behavior of restorative materials. | |
| IV. 1. Introduction..... | 50 |
| IV. 2. Geometry and materials | 50 |
| IV. 3. Finite element analysis..... | 51 |
| IV. 4. Results and discussion | 53 |
| IV. 5. Conclusion | 55 |
| References | 56 |

IV. 1. Introduction

One of the dental restoration problems with porous ceramic materials is the damage they rapidly undergo when they are subjected to monotonic or cyclic thermal loadings, local thermal stresses of high level can develop, sometimes nearby or over the elastic limit, due to the mismatch of elastic and thermal coefficients between the synthetic ceramic and the natural bone materials. For the same reasons, early cracks can appear in restorative materials with multiple layered materials.

Therefore, we aim to rebuild a simplified 3D model to evaluate the thermo-elastic and the elastic behavior of the dental material (natural and prosthesis) in oral cavity, using the thermo-mechanical properties we evaluated in the past chapters.

IV. 2. Geometry and materials

After taking the work of Trindade et al.[1] as reference for this numerical study. A simplified 3D model of premolar tooth is rebuilt, using SOLIDWORKS software.the dimension utilized for this modeling are obtained from the same work and illustrated in the **Figure IV. 1.**

Chapter. IV Numerical 3D modeling of the thermo-elastic behavior of restorative materials.

The model complete mesh consists of 36019 Tetrahedron domain elements, **Figure IV. 2.**

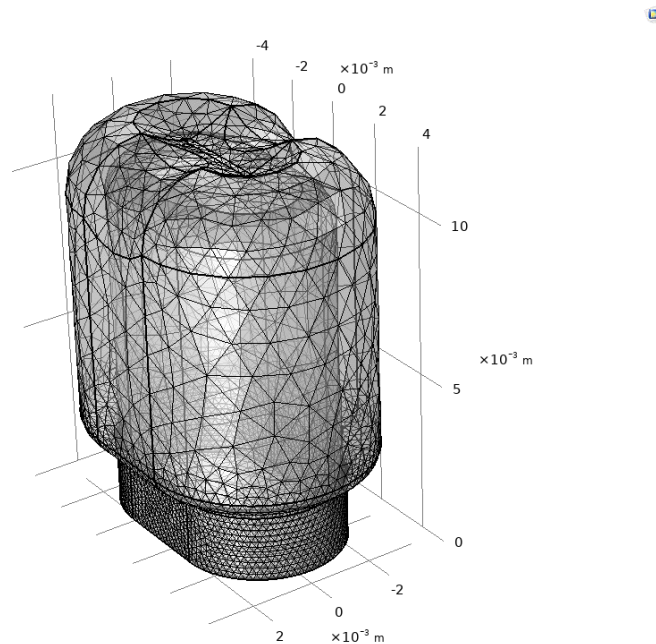


Figure IV. 2. Complete mesh of the simplified tooth model.

The model was loaded with pressure load at shows in

Figure IV. 3 with a magnitude of 50.6 (MPa), which imitates the force of biting to a cylindrical ball of 6 mm in radius with the force of 665N. this value is equivalent to the maximum normal bite force on premolars according to Trindade et al[1]. The nodes at the bottom of the model were fixed, with no movement allowed in any direction. this protocol is made to evaluate the mechanical behavior of the model, **Figure IV. 3.**

In contrast, to evaluate the thermo-mechanical behavior of the same model a uniform thermal load of 80 C° and 37 C° was submitted to the outer shell and the inner core, respectively. **Figure IV. 4.**

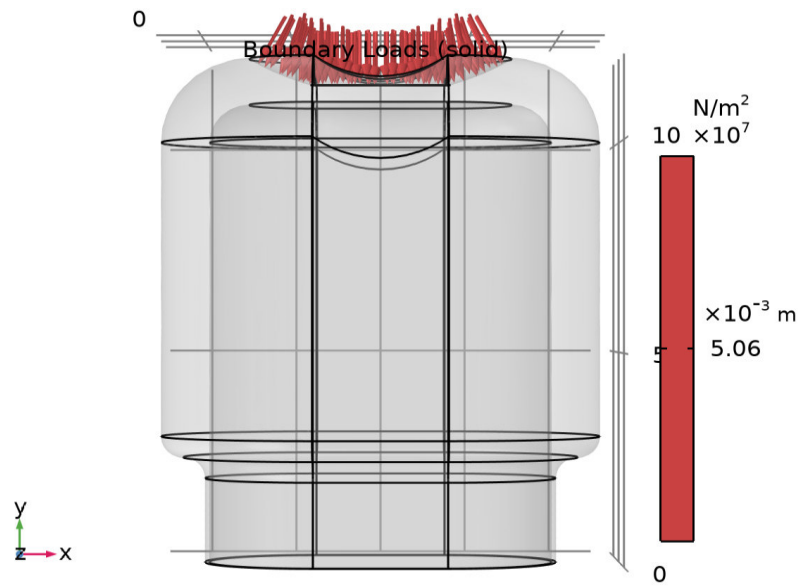


Figure IV. 3. The simplified tooth model Under boundary load.

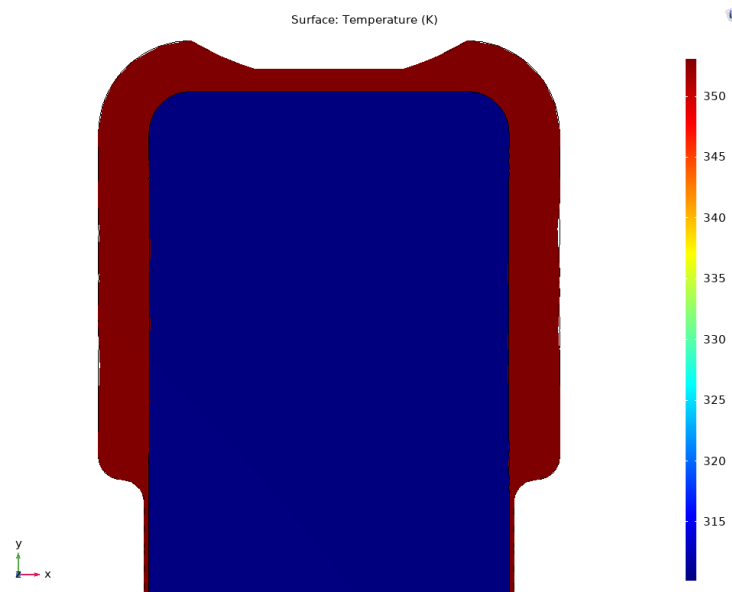


Figure IV. 4. The simplified tooth model Under thermal boundary conditions.

IV. 4. Results and discussion

The results were evaluated in a cross-section in the XY plane, which consists of Von Mises's stress contours. This choice is due to the absence of the proper failure theory evaluation for brittle materials (coulomb-Mohr or maximum principal stress failure theory) in the COMSOL software.

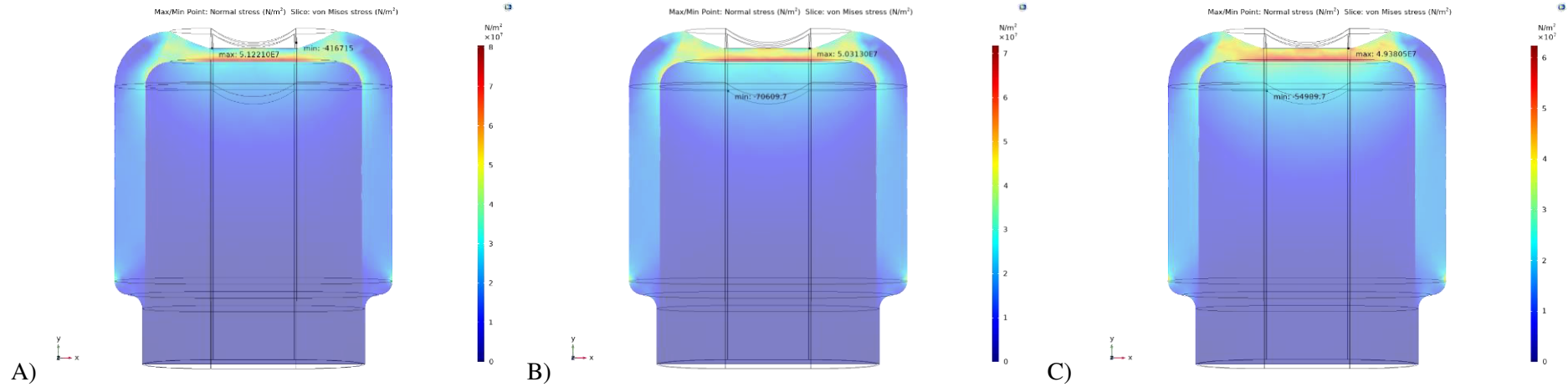


Figure IV. 5. Slice evaluation of Von Mises A) Natural enamel B) IPS e.max CAD C) IPS d.SIGN for Mechanical loading.

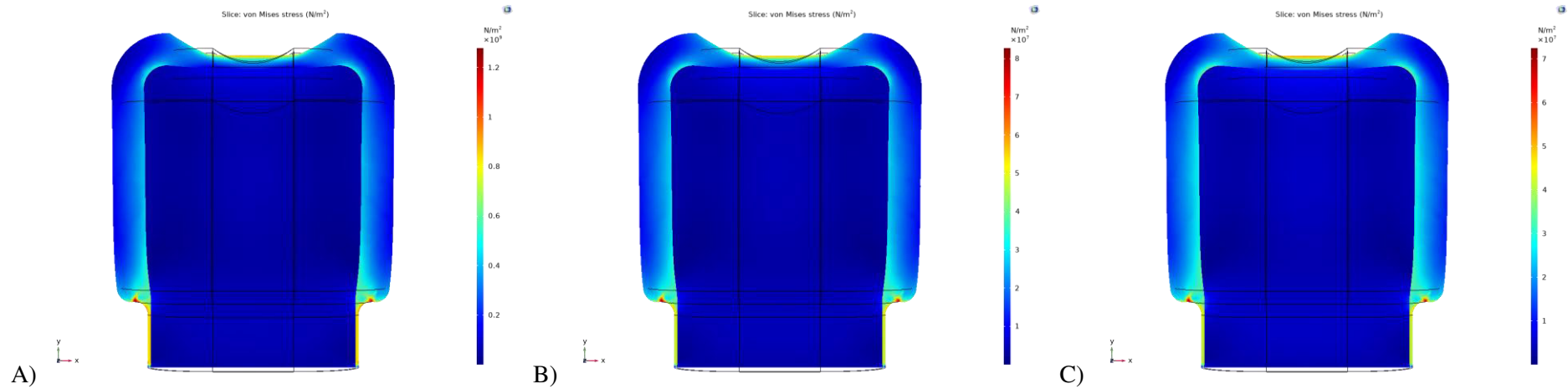


Figure IV. 6 Slice evaluation of Von Mises A) Natural enamel B) IPS e.max CAD C) IPS d.SIGN for thermal loading.

Chapter IV. Numerical 3D modeling of the thermo-elastic behavior of restorative materials.

In the Figure IV. 5 we observe a high concentration of stresses in the outer shell through 3 materials opposite to the inner core. Evaluating the maximum normal stress in all 3 models and comparing it to the work of Trindade et Al[1] demonstrate a good agreement in the results. We also observe higher concentration of stresses in contact region between the outer shell and the inner core, that's due to sudden change in the materials properties. And a peak in the upper region was expected because it consists of a thinned layer. We note a rise in size for the same construction region accompanied with the decreases of the elastic properties of the outer shell (95, 83 and 64 GPa).

For the thermal simulation, we note that the stress concentration caused by the thermal expansion is located in the thinner parts of the outer shell and bonding surface between the inner and the outer body.

IV. 5. Conclusion

Based on our findings and the current study, we came to this conclusion:

- Variation in the elastic properties of out layer influence the stress concentration region, for lower elastic modules a higher stress concentration is noted.
- The elevation in the elastic properties of the used material in the outer layer causes a higher stress concentration at the bonding interfaces.
- The stress concentration in the thermal expansion accurse in the zones of thinner walls and the bonding reign between the two cores.
- The CTE is the largest contributor to the elevation in stress concentration.

References

1. Trindade, F.Z., et al., *Elastic properties of lithium disilicate versus feldspathic inlays: effect on the bonding by 3D finite element analysis*. Journal of Prosthodontics, 2018. **27**(8): p. 741-747.
2. Hengchang, X., L. Wenyi, and W. Tong, *Measurement of thermal expansion coefficient of human teeth*. Australian dental journal, 1989. **34**(6): p. 530-535.
3. Vivadent, I., *IPS d.SIGN Instructions for Use*, 2008: Liechtenstein. p. 68.

General Conclusion

The present work is developed as part of the end-of-study project for the Master's degree in mechanical engineering. The aim of the work is a contribution to the numerical and experimental modeling of the thermo-elastic behavior of materials based upon porous textures where an application to dental restoration materials is considered.

The first part is devoted to the experimental modeling. An experimental protocol was respected for assuring some mechanical and chemical characterization for both natural and dental prosthesis (natural tissue and IPS d.SIGN), respectively. This approach is adopted to assess the mechanical behavior of the materials and to give more information about crystalline phases.

The second part is dedicated to the numerical modeling of the thermo-elastic behavior of two kinds of materials; glass-ceramic introduced in the experimental part and also the IPS e.max CAD. In addition to the analytical approach of Mori-Tanka, numerical method (Finite Elements) was used simultaneously in evaluating the equivalent homogeneous properties of different glass-ceramic microstructures, all numerical developments take in account the porous aspect of the microscopic using a tomography technique.

In order to evaluate the thermo-mechanical behavior and properties, the deduced results are used in 3D simplified modeling of premolar tooth imitating the use of dental restoration materials as substitution of the natural tooth.

Based on the whole of the current study, we can summarize the following conclusions:

- Dentin microstructure variation has a direct effect on mechanical properties of the tooth.
- In general, porosity has some effects on the elastic properties of the micro-structural material and does not affect the coefficient of thermal expansion.
- In addition to the geometric morphology of tooth, elastic properties of outer shell have a significant influence on the stress concentration region.
- High elastic properties of the used material in outer shell cause a higher stress concentration at the bonding interfaces.

The present work has revealed some perspectives; among them we recommend on one hand, an experimental investigation regarding the porosity effects on Poisson's ratio and CTE of glass-ceramic material, and further detailed chemical analysis, on the other hand.

Abstract

As part of the study of the effect of porosity on the thermo-elastic behavior of mineral materials, two aspects are addressed. First, an experimental analysis based on mechanical and chemical characterization was carried out on both natural dental tissues and IPS d.SIGN glass-ceramics, intended for dental restoration. Second, two numerical and analytical approaches; Finite Element and Mori-Tanaka, respectively, have been adopted to model the same behavior, where IPS d.SIGN and IPS e.max (CAD) glass-ceramics are used. The coefficient of thermal expansion as well as the elastic properties of the homogenized materials are obtained and exploited in a numerical modeling of a virtual structure of a natural tooth.

Keywords: Finite element method, Mori-Tanaka method, Representative Elementary Volume, Porous materials, Glass-ceramics.

Résumé

Dans le cadre d'étude de l'effet de la porosité sur le comportement thermo-élastique des matériaux minéraux, deux aspects ont été traités. Premièrement, une analyse expérimentale visant la caractérisation mécanique et chimique a été effectuée sur des tissus dentaires d'une part et de vitrocéramique IPS d.SIGN, destinés à la restauration dentaire, d'autre part. Deuxièmement, deux approches numérique et analytique ; Elément Finis et de Mori-Tanaka, respectivement, ont été adoptées à la modélisation du même comportement, dont les vitrocéramiques IPS d.SIGN et IPS e.max (CAD) sont utilisés. Le coefficient de dilatation thermique ainsi que les propriétés élastiques des matériaux homogénéisés sont obtenus et exploités dans une modélisation numérique d'une structure d'un prototype de dent naturelle.

Mots clés : Méthode des éléments finis, Méthode Mori-Tanaka, Volume Élémentaire Représentatif, Matériaux poreux, Vitrocéramique.

المخلص

في إطار دراسة تأثير المسامية على سلوك المرونة الحرارية للمواد المعدنية، تم تناول جانبين. أولاً ، تم إجراء تحليل تجريبي يهدف إلى تحديد الخصائص الميكانيكية والكيميائية لكل من أنسجة الأسنان الطبيعية و السيراميك الزجاجي IPS d.SIGN ، المخصص لترميم الأسنان. ثانياً، تم اعتماد منهجيتين عدديتين وتحليلية ؛ العناصر المنتهية و موري-تانكا، على التوالي، لنمذجة نفس السلوك، حيث تم استخدام السيراميك الزجاجي IPS d.SIGN و IPS e.max CAD كمواد مشكلة. تم الحصول على معامل التمدد الحراري وكذلك الخصائص المرنة للمواد المتجانسة واستغلالها في النمذجة العددية للبنية الافتراضية للسن الطبيعي.

الكلمات المفتاحية: طريقة العناصر المحدودة ، طريقة موري تانكا ، عنصر الحجم التمثيلي ، المواد المسامية ، السيراميك الزجاجي.

Acknowledgements

We would like to acknowledge and give Our warmest thanks to our supervisor Pr.Lakhder SEDIRA, who made this work possible. His guidance and advice carried us through all the stages of writing our project. And the help of the other teachers with their knowledge especially Dr. Belhi GUERIRA and Dr.Rachid MAKHLOUFI.

Major thanks to Mr. Badreddine GASSIRI without him this project will never be possible for his knowledge and experience in the domain never forgetting the help provided by him.

we would also like to give special thanks to our long-life friends Abd-Latif SEGHEIRI and Salim BOUDIAF for their continuous support and understanding when undertaking my research and writing my project. Your prayer for me was what sustained me this far.

Never forgetting the new friendships, we have established in my path of knowledge, To Mohamed-Elamine GUERBAZI and Anfel Laribi. Thank you for making our trip full of joy and happiness, and may Allah bring us to gather as co-workers in this career.

we would be remiss in not mentioning Kaltoum MOKRANI for making our study experience unforgettable.

Finally, we would like to thank Allah, for letting us through all the difficulties. We have experienced your guidance day by day. You are the one who let me finish my degree. we will keep on trusting you for our future.

Ayoub MACHIOURI

Manar GUITOUN